

Upper crustal deformation in continent-continent collision: A case study from the Bernard nappe complex (Valais, Switzerland)

Thomas Scheiber,¹ O. Adrian Pfiffner,² and Guido Schreurs²

Received 13 November 2012; revised 16 July 2013; accepted 30 August 2013; published 3 October 2013.

[1] The Penninic nappes in the Swiss Alps formed during continental collision between the Adriatic and European plates in Cenozoic times. Although intensely studied, the finite geometry of the basement-bearing Penninic nappes in western Switzerland has remained a matter of debate for decades (e.g., “Siviez-Mischabel dilemma”) and the paleogeographic origin of various nappes has been disputed. Here, we present new structural data for the central part of the Penninic Bernard nappe complex, which contains pre-Permian basement and Permo-Mesozoic metasedimentary units. Our lithological and structural observations indicate that the discrepancy between the different structural models proposed for the Bernard nappe complex can be explained by a lateral discontinuity. In the west, the presence of a Permian graben caused complex isoclinal folding, whereas in the east, the absence of such a graben resulted mainly in imbricate thrusting. The overall geometry of the Bernard nappe complex is the result of three main deformation phases: (1) detachment of Mesozoic cover sediments along Triassic evaporites (Evolène phase) during the early stages of collision, (2) Eocene top-to-the-N(NW) nappe stacking (Anniviers phase), and (3) subsequent backfolding and backshearing (Mischabel phase). The southward localized backshearing is key to understand the structural position and paleogeographic origin of units, such as the Frilhorn and Cimes Blanches “nappes” and the Antrona ophiolites. Based on these observations, we present a new tectonic model for the entire Penninic region of western Switzerland and discuss this model in terms of continental collision zone processes.

Citation: Scheiber, T., O. A. Pfiffner, and G. Schreurs (2013), Upper crustal deformation in continent-continent collision: A case study from the Bernard nappe complex (Valais, Switzerland), *Tectonics*, 32, 1320–1342, doi:10.1002/tect.20080.

1. Introduction

[2] The Alpine orogenic belt is a classical area for the study of continental collision zone processes. Subduction, collision, and exhumation of continental and oceanic fragments between the European and Adriatic plates involved intricate deformation and resulted in highly complex nappe structures [e.g., Schmid *et al.*, 2004]. Revealing the final geometry and structural evolution of these various continental and oceanic nappes is crucial to develop conceptual models for the evolution of continental collision zones in general. Despite at least a century of geological research, many fundamental questions related to the final geometry and the processes, which led to this geometry as well as the paleogeographic origin of many Alpine nappes, are still open or debated.

[3] A classical example for such a debate is the Penninic zone of western Switzerland (Figure 1), where three fundamental questions regarding the evolution of the Alpine orogenic belt have remained open:

[4] 1. The “Siviez-Mischabel dilemma”: Are the intercalations of crystalline basement and cover rocks formed by recumbent folds or by thrust faults? In the classical model of Argand [1909, 1916], the Siviez-Mischabel nappe represents a large-scale, isoclinal, basement-cored, recumbent, and north-vergent fold, surrounded by Permo-Triassic sediments. This model has been strongly supported by, for example, Thélin [1987], Escher [1988], Escher *et al.* [1988, 1993, 1997], Thélin *et al.* [1993], Epard and Escher [1996], Escher and Beaumont [1997], and Genier *et al.* [2008]. In contrast, Staub [1937], Jäckli [1950], and Markley *et al.* [1999] proposed that the Siviez-Mischabel nappe, at least in its frontal part, consists mainly of thrust sheets, which were placed on top of each other without the development of a large-scale overturned fold limb. These conflicting models nicely illustrate the contrasting views among geoscientists and raise fundamental questions on the formation of basement-bearing nappes under low-grade metamorphic conditions in continental collision zones.

[5] 2. How important is top-to-the-west, orogen-parallel shearing? Previous studies within the area have been at odds with each other regarding the importance of top-to-the-west orogen-parallel shearing. Several studies proposed the existence of large-scale top-to-the-west shear zones in the entire area [e.g., Sartori *et al.*, 2006; Sartori and Epard, 2011] whereas others did not observe such large-scale shear zones [e.g., Escher *et al.*, 1997; Genier *et al.*, 2008].

¹Norwegian Geological Survey (NGU), Trondheim, Norway.

²Institute of Geological Sciences, University of Bern, Switzerland.

Corresponding author: T. Scheiber, Norwegian Geological Survey (NGU), Leiv Eirikssons vei 39, 7040 Trondheim, Norway. (thomas.scheiber@ngu.no)

©2013. American Geophysical Union. All Rights Reserved. 0278-7407/13/10.1002/tect.20080

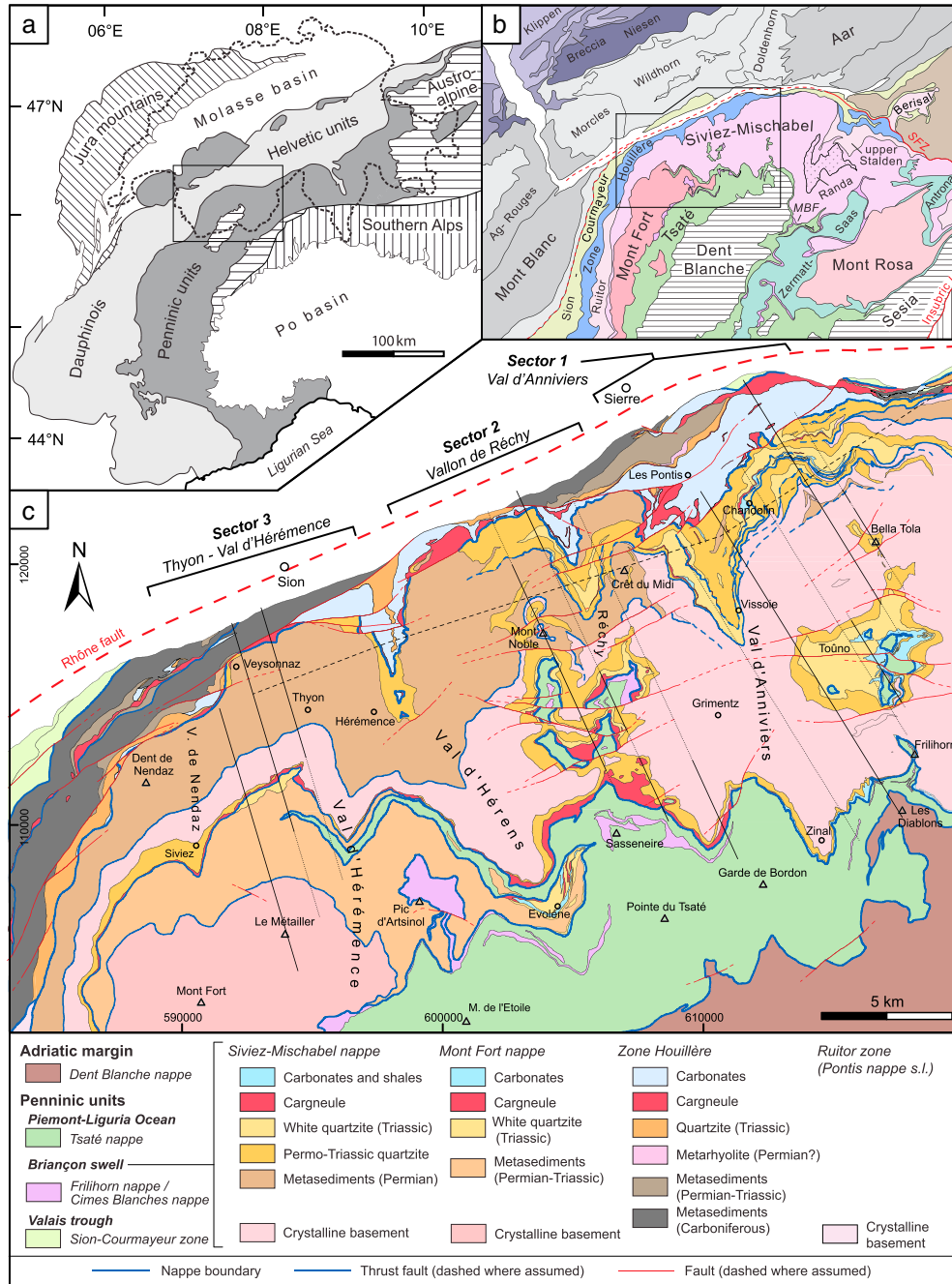


Figure 1. (a) Tectonic sketch map of the Central and Western Alps. Rectangle indicates location of Figure 1b. (b) Larger tectonic framework of the study area (location indicated by polygon). Penninic units are colored with the same color scheme used in Figure 12. *MBF* indicates the location of the Mischabel backfold, *SFZ* the location of the Simplon Fault Zone. (c) Geological map of the study area based on maps of the Geological Atlas of Switzerland, i.e., sheet Sierre [Gabus *et al.*, 2008a], Vissoie [Marthaler *et al.*, 2008a], and Sion [Sartori *et al.*, 2011], on tectonic map compilations of Escher [1988] and Steck *et al.* [1999], on work of Schaer [1959], Allimann [1987], and own observations. Main tectonic units are listed in the legend according to their paleogeographic origin. Lithological information is only provided for Briançon-derived units. The study area is divided into three sectors (see text). Traces of compiled cross sections (Figure 5) are continuous where shown in the profiles and dotted where not shown in the profiles but used for construction. The dashed black line marks the trace of the ENE-WSW cross section shown in Figure 10. Coordinates are in the Swiss National Grid. Integrated with Figure 1c: Buxtorf, A., and E. Wegmann (unpublished map, 1923), Geologische Karte der Zuleitungs- und Druckleitungs-Strecken im Val d'Hérens und Val d'Hérémence, scale 1:50,000, available from Hydro Exploitation SA, Sion.

[6] 3. What is the paleogeographic origin of tectonic units like the Frilhorn, Cimes Blanches, and Monte Rosa nappes as well as the Antrona ophiolites (Figure 1), and which processes led to their actual position within the nappe stack? Various contrasting models have been proposed for these units, and no consensus about the pre-Alpine paleogeographic position has been reached so far [e.g., *Ballèvre and Merle*, 1993; *Escher et al.*, 1997; *Stampfli et al.*, 1998; *Froitzheim*, 2001; *Froitzheim et al.*, 2006; *Keller and Schmid*, 2001; *Marthaler et al.*, 2008b].

[7] In the following study we address these fundamental questions by investigating the structural geometry and tectonic evolution of the central Bernard nappe complex in western Switzerland (Figure 1). Based on structural field mapping, we present cross sections and develop a 3-D model for the area. We then discuss the issues raised above and place our results in a larger tectonic framework for the Penninic nappes of the Swiss Alps. These results help to constrain and understand the processes acting in continental collision zones in general.

2. Geological Setting

2.1. Tectonic Framework

[8] The Bernard nappe complex (“Nappe du Grand St-Bernard” in the sense of *Argand* [1909] and “Grand St. Bernard nappe system” after *Schmid et al.* [2004]) is part of the Penninic nappe system of the Western and Central Alps, which extends geographically from eastern Switzerland westward and southward all the way to the Ligurian Sea (Figure 1a).

[9] In western Switzerland, the Bernard nappe complex has traditionally been subdivided into four tectonic units, from structurally lowest to highest (Figure 1b): Zone Houillère, Pontis nappe (including Ruitor zone, upper Stalden zone and Berisal unit), Siviez-Mischabel nappe, and Mont Fort nappe [*Escher*, 1988; *Escher et al.*, 1988, 1997; *Steck et al.*, 1999, 2001]. The Permian to Triassic rocks of the Pontis nappe, however, are now regarded as part of the Zone Houillère [e.g., *Sartori et al.*, 2006].

[10] The different tectonic units of the Bernard nappe complex are attributed to the Briançon paleogeographic realm [*Ellenberger*, 1952; *Sartori*, 1987a; *Stampfli*, 1993]. According to reconstructions of the Cretaceous paleogeography the Briançon swell represented a piece of thinned European continental crust that separated two basins: the Valais trough to the north and the Piemont-Liguria Ocean to the south, which in turn were bordered by the continental margins of the European and Adriatic plates, respectively [*Stampfli et al.*, 1998; *Schmid et al.*, 2004].

[11] Today, the Bernard nappe complex is sandwiched between relics of these two basin domains and constitutes the Middle Penninic nappe system (Figures 1b and 1c). In the north, the Zone Houillère is thrust on top of the Lower Penninic Sion-Courmayeur zone, which comprises remnants of the former Valais trough (Figures 1b and 1c) [e.g., *Trümpy*, 1951; *Jeanbourquin and Burri*, 1991]. Along the central Rhône valley the units are transected by the dextral Rhône fault, which is interpreted as the prolongation of the brittle detachment along the Simplon Fault Zone (Figure 1b) [e.g., *Steck*, 1984]. The Simplon Fault Zone (in the sense of *Campani et al.* [2010]) juxtaposes greenschist facies rocks of the Bernard nappe complex against amphibolite facies rocks

of the Lepontine dome and is characterized by a broad ductile mylonite zone in the footwall, separated by a discrete brittle detachment from the little affected hanging wall, and was active from circa 20 Ma onward [e.g., *Mancktelow*, 1985; *Campani et al.*, 2010]. To the south, upper Penninic units derived from the Piemont-Liguria Ocean tectonically overlie the Bernard nappe complex (Figures 1b and 1c). In our study area, they are represented by the Tsaté nappe, which comprises Late Jurassic to Cretaceous metasedimentary rocks such as calcschists and black shales (“schistes lustrés”) and prasinites, mainly derived from basalts but also from gabbros [*Sartori*, 1987a; *Marthaler and Stampfli*, 1989; *Deville et al.*, 1992]. Within and at the base of the Tsaté nappe units consisting of terrestrial and shallow marine rocks occur, which have been given different local names (e.g., “Oberer Würmlizug” [*Witzig*, 1948], Frilhorn series [*Marthaler*, 1984; *Sartori*, 1987a], Cimes Blanches series [*Vannay and Allemann*, 1990], “Serie d’Evolène” [*Escher*, 1988], or Berté unit [*Allimann*, 1989]) but which are now generally known as the Frilhorn and Cimes Blanches nappes (Figure 1c) [e.g., *Steck et al.*, 2001; *Sartori et al.*, 2006]. The internal stratigraphy of these nappes resembles the one found in the Klippen and Breccia nappes of the Préalpes (Figure 1b), but—as mentioned earlier—the origin of these continental sediments is still under debate [e.g., *Escher et al.*, 1997; *Froitzheim et al.*, 2006; *Sartori et al.*, 2006; *Pleuger et al.*, 2007]. The Tsaté, Frilhorn, and Cimes Blanches nappes are collectively known as the Combin zone [see *Lebit et al.*, 2002, Table 1]. Farther to the southeast, the upper Penninic Zermatt-Saas and Antrona ophiolites envelop the Monte Rosa nappe (Figure 1b). The Monte Rosa crystalline basement resembles the crystalline basement of the Bernard nappe complex, but its paleogeographic position relative to the Bernard nappe complex is debated [*Froitzheim*, 2001 and references therein]. U/Pb zircon ages from the Zermatt-Saas and Antrona ophiolites are typical for the Piemont-Liguria Ocean (166–148 Ma [*Liati et al.*, 2003; 2005]). Finally, the Dent Blanche nappe—part of the former Adriatic continental margin (Austroalpine in Figure 1a)—rests on top of the entire nappe pile (Figures 1a–1c). In the Valle d’Aosta region, crystalline basement units with Austroalpine-affinity occur also as slivers between the Zermatt-Saas zone and the Tsaté nappe [e.g., *Ballèvre and Merle*, 1993; *Beltrando et al.*, 2010].

2.2. Lithostratigraphy of the Bernard Nappe Complex in the Valais

[12] For a detailed description of the lithostratigraphy of the various tectonic units of the Bernard nappe complex, the reader is referred to *Sartori et al.* [2006]. Here we restrict ourselves to a brief description of those lithologies, which are particularly relevant for our study area (Figure 1c).

[13] The Zone Houillère is mainly characterized by Late Paleozoic to Mesozoic continental deposits such as sandstones, metaconglomerates, and black shales [*Gabus et al.*, 2008b; *Sartori and Eparard*, 2011]. In the western part of the study area, the Zone Houillère is divided by a tectonic mélange mainly composed of cagneule into a northern external and a southern internal part (Figure 1c) [*Thélin et al.*, 1993]. In the eastern part of the study area, the Zone Houillère contains Triassic quartzites, cagneule, and carbonates, plus the Permian to Triassic rocks of the former Pontis

nappe [Sartori *et al.*, 2006]. The crystalline basement of the Zone Houillère is not known.

[14] The Siviez-Mischabel nappe constitutes the biggest part of the Bernard nappe complex exposed in the study area (Figure 1c). It consists of polymetamorphic basement and monometamorphic (mainly) sedimentary rocks. The polymetamorphic basement is made up of a variety of paragneisses and micaschists, interlaced with amphibolite and minor eclogite bodies [Sartori and Thélin, 1987; Thélin *et al.*, 1990; Rahn, 1991]. It also contains minor metaigneous rocks such as metagranites [Bussy *et al.*, 1996a] and metagabbros [Sartori, 1990]. The monometamorphic lithologies can be grouped into five main units: (1) Permian sediments containing mainly quartz-rich conglomerates, schists, metavolcaniclastics, and metapelites [Vallet, 1950; Schaer, 1959; Burri, 1983]. (2) Small granitic bodies and dikes associated with the post-Variscan (269 ± 2 Ma) Randa orthogneiss [Bearth, 1963; Thélin, 1987; Bussy *et al.*, 1996b; Genier *et al.*, 2008]. The main body of this intrusion is located east of the study area (Figure 1b). The small granitic bodies locally intrude polymetamorphic basement and Lower Permian sediments. (3) (Permo-Triassic) quartzites that lie either stratigraphically on top of the Permian sediments or directly on top of crystalline basement units. (4) In many areas, cargneule overlies the Permo-Triassic quartzite and represents an important detachment horizon during Alpine tectonics [Schaad, 1995]. (5) In the eastern part of the study area, fragments of the mainly Mesozoic and dominantly carbonatic sequence still rest on top of the quartzites (Figure 1c). They are known as Barrhorn and Toûno series [cf. Ellenberger, 1953; Sartori, 1987b]. Early descriptions of these series can be found in Hermann [1913] and Göksu [1947]. The stratigraphy of these units is correlated with the one observed in the Klippen nappe farther north in the Préalpes (Figure 1b) [e.g., Sartori *et al.*, 2006] and can in parts also be recognized in the Frilihorn nappe [Sartori, 1987a] and in the Cimes Blanches nappe [e.g., Vannay and Allemann, 1990]. However, the Frilihorn and Cimes Blanches nappes are usually regarded as analogues to the Breccia nappe, which lies on top of the Klippen nappe [e.g., Sartori *et al.*, 2006]. In any case, both the Klippen and Breccia nappes of the Préalpes have been interpreted as representing the sheared-off cover from the Siviez-Mischabel and related nappes [e.g., Lemoine, 1960; Baud and Septfontaine, 1980; Sartori *et al.*, 2006].

[15] The Mont Fort nappe is the tectonically highest unit and only appears in the western part of the study area (Figures 1b and 1c). Its pre-Permian basement is collectively known as Métailler unit and is made up of micaschists and gneisses containing mafic components such as pillow lavas and gabbros [Schaer, 1959]. This basement was regarded as monometamorphic by several authors [e.g., Allimann, 1987; Thélin *et al.*, 1993; Gouffon and Burri, 1997], but recent studies suggest an early Paleozoic age for the protoliths of this unit [Sartori *et al.*, 2006; Gauthiez *et al.*, 2011], which makes a polymetamorphic evolution probable. A series of Permian to Triassic sediments is regarded as the cover of the Mont Fort basement and consists mainly of metaconglomerates, -arkoses, and -sandstones, occasionally with a considerable proportion of slates [Wegmann, 1923; Schaer, 1959; Allimann, 1987]. A few relict carbonates of the Mont Fort cover are preserved near Evolène (Figure 1c).

Cargneules mark the tectonic contact between the Siviez-Mischabel and Mont Fort nappes.

2.3. Metamorphic History and Radiogenic Isotope Data

[16] The monometamorphic sequences of the Bernard nappe complex show a greenschist facies Alpine metamorphic overprint [Bousquet *et al.*, 2004; Oberhänsli *et al.*, 2004], with the metamorphic grade increasing toward structurally higher units and reaching high-P greenschist facies in meta-argillites of the Barrhorn series [Sartori, 1990; Chopin *et al.*, 2003]. The overlying Mont Fort and Tsaté nappes experienced upper greenschist to blueschist facies conditions reaching maximum circa 900 MPa and 300–450°C [Bearth, 1963; Reddy *et al.*, 2003]. Farther south, the Zermatt-Saas zone, together with the Antrona ophiolites and the Monte Rosa nappe, experienced Alpine eclogite facies overprint [Lapen *et al.*, 2003; Bousquet *et al.*, 2004; Frezzotti *et al.*, 2011]. A metamorphic gap and thus a clear tectonic contact separates the Combin zone from the underlying Zermatt-Saas zone (Figure 1b) [Ballèvre and Merle, 1993; Ring, 1995; Pleuger *et al.*, 2007].

[17] The Alpine eclogite facies metamorphism is dated at circa 44 Ma for the Zermatt-Saas zone [Rubatto *et al.*, 1998], circa 40 Ma for the Monte Rosa nappe [Lapen *et al.*, 2007], and circa 38 Ma for the Antrona ophiolites [Liati *et al.*, 2005]. Rb/Sr data from micas along the tectonic contact between the Zermatt-Saas and the Combin zones give crystallization ages of 42–37 Ma [Cartwright and Barnicoat, 2002] and 45–36 Ma with an age peak at around 37 Ma [Reddy *et al.*, 1999, 2003], coeval to slightly younger than the high-pressure metamorphism. The formation of the Bernard nappe complex within the study area is constrained by $^{40}\text{Ar}/^{39}\text{Ar}$ ages of synkinematically grown micas, which were dated at 41–36 Ma [Markley *et al.*, 1998, 2002]. Roughly the same $^{40}\text{Ar}/^{39}\text{Ar}$ ages were obtained from micas both within the basement and cover rocks easterly adjacent to the study area [Hunziker and Bearth, 1969; Hunziker, 1969; Barnicoat *et al.*, 1995], indicating a relatively short time span of metamorphism and ductile deformation within the entire Penninic nappe stack of western Switzerland.

[18] The metamorphic history of the polymetamorphic basement of the Bernard nappe complex is complex and not entirely resolved yet. K/Ar dating [Soom, 1990] and $^{40}\text{Ar}/^{39}\text{Ar}$ dating [Markley *et al.*, 1998; Kramar *et al.*, 2001] of white mica populations from the Siviez-Mischabel basement, which in most cases define the dominant foliation developed under greenschist facies conditions, predominantly yield Permo-Carboniferous ages. This suggests that the main foliation and greenschist facies metamorphism in the basement are associated with the Variscan orogeny and that Alpine metamorphic overprint was minor in these basement units. Similar ages are reported from relict amphibolite facies assemblages of the Ruitor zone [Thélin and Ayrton, 1983; Giorgis *et al.*, 1999]. An amphibolite facies metamorphic event—older than the greenschist facies overprint described above—is recognized within several basement units of the Bernard nappe complex [Bearth, 1963; Thélin *et al.*, 1993]. In addition, mafic bodies host lenses with preserved eclogitic paragenesis that predate the amphibolite facies metamorphism [e.g., Thélin, 1989; Thélin *et al.*, 1993]. However, the absolute timing of these metamorphic events is not well constrained. For the eclogites from the Siviez-Mischabel nappe a Cambro-Ordovician age was proposed

[Thélin *et al.*, 1990; Eisele *et al.*, 1997], whereas eclogites from the Briançon basement of the western Alps were interpreted as Proterozoic in age [e.g., Desmons, 1992; Desmons *et al.*, 1999].

2.4. Previous Structural Work and Tectonic Models

[19] Different tectonic models exist for the polyphase deformation history of the Bernard nappe complex of the Valais region in western Switzerland. In the explanations to the 1:25,000 map sheets Sierre, Vissoie, and Sion of the Geological Atlas of Switzerland (Gabus *et al.* [2008b], Marthaler *et al.* [2008b], and Sartori and Eparad [2011], respectively) a deformation history consisting of four main deformation phases is proposed: during D1, northward directed nappe stacking took place. During D2, top-to-the-WSW shearing along discrete subhorizontal shear zones occurred, which shows similar kinematics as the Simplon ductile shear zone in the sense of Steck [1990] but which was active earlier and at higher structural levels (see Figure 2 in Sartori *et al.* [2006]). D3 describes a phase of postnappe back-folding, and D4 is a brittle deformation stage, related to the Simplon-Rhône fault.

[20] Genier [2007] presents a deformation scheme for the Randa orthogneiss and surrounding units east of our study area. He observed no evidence for the D2 postnappe top-to-the-WSW shear zones of Sartori *et al.* [2006] but interpreted NE-SW oriented stretching lineations as extensional structures related to the Simplon ductile shear zone, as introduced by Steck [1984, 1990]. Pleuger *et al.* [2008] report D2 orogen-parallel extension with a top-to-the-SW shear sense—the local Malfatta phase—from the SW Monte Rosa nappe.

[21] Milnes *et al.* [1981] defined four deformation phases for the Penninic nappe system in western Switzerland: Top-to-the-NW thrusting is followed by a phase of isoclinal folding with the same kinematics (Ragno-Randa phase). The resulting structures are overprinted by two distinct phases of backfolding (Mischabel phase and Vanzone phase). The structure of the Mischabel backfold (Figure 1b) was extensively studied by Müller [1983]. He observed evidence for backshearing and suggested a block-shear model to explain the backfolding (Mischabel phase after Milnes *et al.* [1981]). Complex deformation and overprinting patterns during a “backthrusting event” are also reported from phyllitic calcschists within the Tsaté nappe of Val d’Hérens [Savary and Schneider, 1983]. Approaching the Monte Rosa nappe and the Southern Steep Belt of the Alps, structures related to an additional phase of backfolding (Vanzone phase after Milnes *et al.* [1981]) become more prominent [e.g., Kramer, 2002; Pleuger *et al.*, 2008].

[22] Bucher *et al.* [2004] studied the deformation history of the Briançon domain in the prolongation of the Bernard nappe complex SW of our study area and considered three main deformation phases to be responsible for the finite geometry of the investigated nappes: D1 and D2 top-to-the-NW nappe stacking followed by D3 backfolding. No top-to-the-SW shearing phase is described in this study.

[23] Our review of previous studies indicates that top-to-the-N(NW) nappe emplacement and later backfolding have been observed throughout the region, whereas evidence for intermediate top-to-the-WSW shearing seems to be restricted to certain areas.

3. Structural Architecture of the Central Bernard Nappe Complex

[24] In order to unravel the structural architecture and deformational history of the central Bernard nappe complex, we investigated three NW-SE trending sectors in the central Valais region (Figure 1c). These sectors were chosen along ridges between major tributary valleys. Our structural study is mainly based on observations from the Siviez-Mischabel nappe but also includes observations from the Zone Houillère, the Mont Fort, Frilhorn, Cimes Blanches, and Tsaté nappes (Figures 1b and 1c). Structural observations were made on macroscopic, mesoscopic, and microscopic scales. We first present representative field examples (Figure 2) and structural data (Figures 3 and 4) from penetrative structures, which occur throughout the entire study area. We then present cross sections (Figure 5) and structural details from each sector (Figures 6 to 9) and close with a presentation and discussion of the large-scale structure of the entire area (Figures 10 to 12).

3.1. Penetrative Structures Present in the Entire Study Area

3.1.1. Basement

[25] All lithologies from the polymetamorphic basement units of the Siviez-Mischabel and Mont Fort nappes from the three investigated sectors contain one dominant tectonic foliation, in the following termed main foliation. This main foliation generally strikes (E)NE-(W)SW (Figure 3a). In the interior of the basement units, far away from contacts to the Permo-Mesozoic, this main foliation is generally steeply dipping. Close to the contacts with the sediments (maximum 50 m distance), it is generally rotated into subparallelism with the overlying parautochthonous sediments (Figure 3a).

[26] The main foliation is affected by at least two folding phase at all scales. The first folds have axial surfaces that systematically dip gently toward the SSE (Figures 2a–2d and 3b). In some cases, an axial planar cleavage is developed (Figures 2b, 2c, and 3b). Toward the contact to the Permo-Mesozoic sediments, these folds become generally more pronounced and the axial planar cleavage locally completely obliterates the preexisting foliation. Fold axes of these folds are subhorizontal and show variable azimuth values but plot mainly in the NE/SW quadrangles (Figure 3b). Stretching lineations on this new foliation are mainly defined by N(NW)-S(SE) aligned quartz and micas but also by disrupted minerals such as tourmaline needles. They are associated with a top-to-the-N(NW) shear sense (Figures 4a and 4d). In places where no new foliation developed, the main foliation is locally intersected by top-to-the-N(NW) shear bands. Locally, a younger phase of folding overprints the SSE dipping axial planar cleavage. These folds are mostly south-vergent and have ENE-WSW trending fold axes and NNW dipping axial planes (Figure 3d). They are particularly well developed in the vicinity of the basement-cover contact.

[27] In addition, porphyroclasts within orthogneisses of the basement are elongated into an ENE-WSW direction, perpendicular to the main stretching lineation on the south dipping main foliation (Figure 4a). There are no shear sense indicators associated with this stretching lineation. Since its direction is coaxial to both the fold axes of the first and second folding generation (Figures 3 and 4), it is difficult to unravel during which phase it formed.

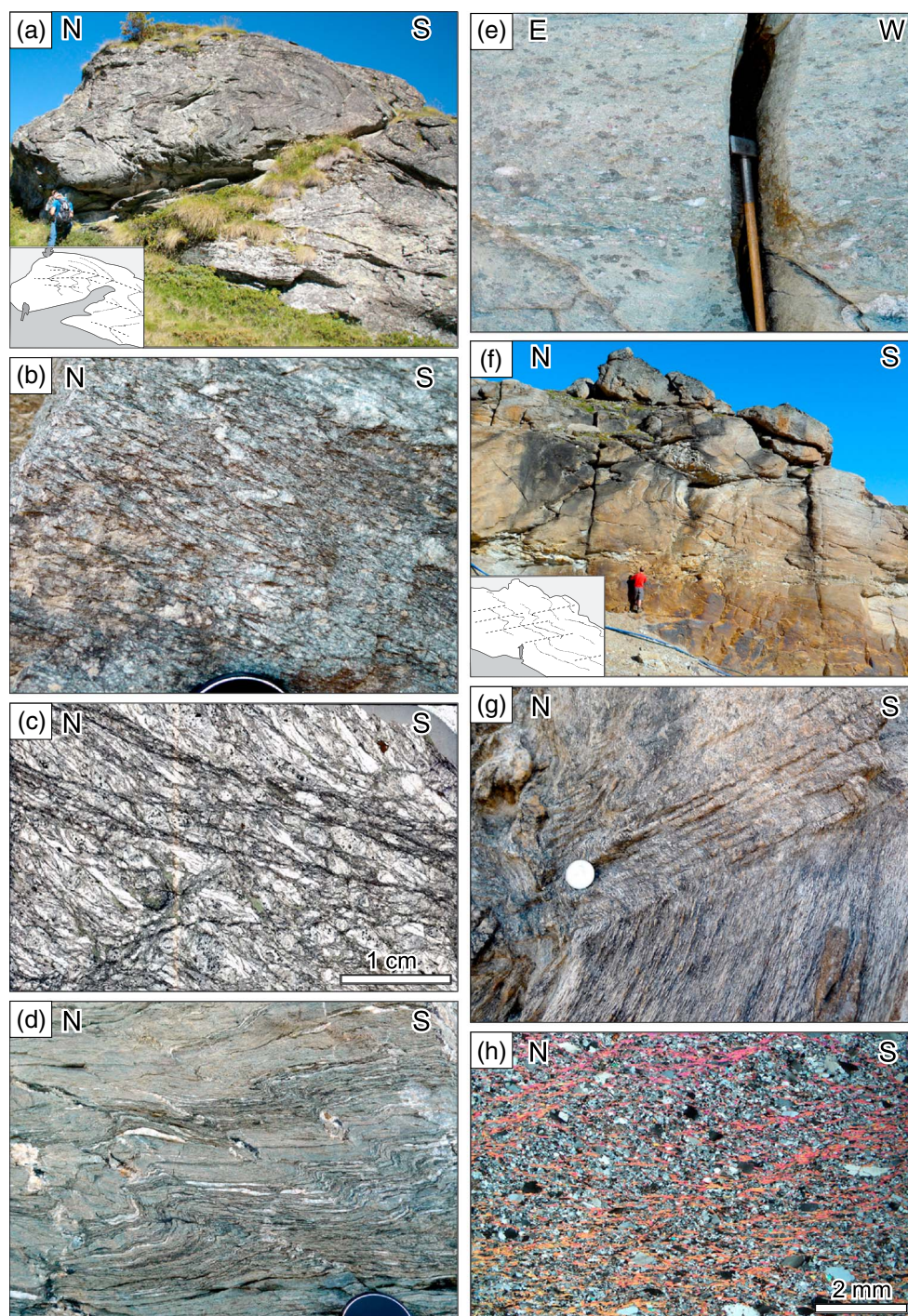


Figure 2. Field aspects of structures at various scales. (a) Basement gneiss folded at mesoscale in the Vallon de Réchy (605353/115875), person for scale. (b) Basement gneiss folded at microscale in the Val d'Anniviers (611809/119884), upper part of lens cover for scale. (c) Discrete shear planes crosscut the main foliation in the basement, which is composed of quartz, feldspar, chlorite, and white mica (thin section scan, 610427/110091). (d) North-vergent folds affect a flat-lying main foliation in the basement (616989/120066). Lens cover for scale. (e) The main foliation in the quartzite is subparallel to sedimentary layering (604962/113558), hammer for scale. (f) The main foliation in the quartzite is folded at outcrop-scale (606149/112540), person for scale. (g) Crenulation cleavage in quartzite, associated with folds, dips toward the NNW (607965/111290), coin for scale. (h) White micas of the main foliation in the quartzite are folded and partly aligned parallel to the crenulation cleavage (617018/114218). In order to present all photographs in the same orientation, Figures 2a, 2b, 2d, and 2f were flipped horizontally.

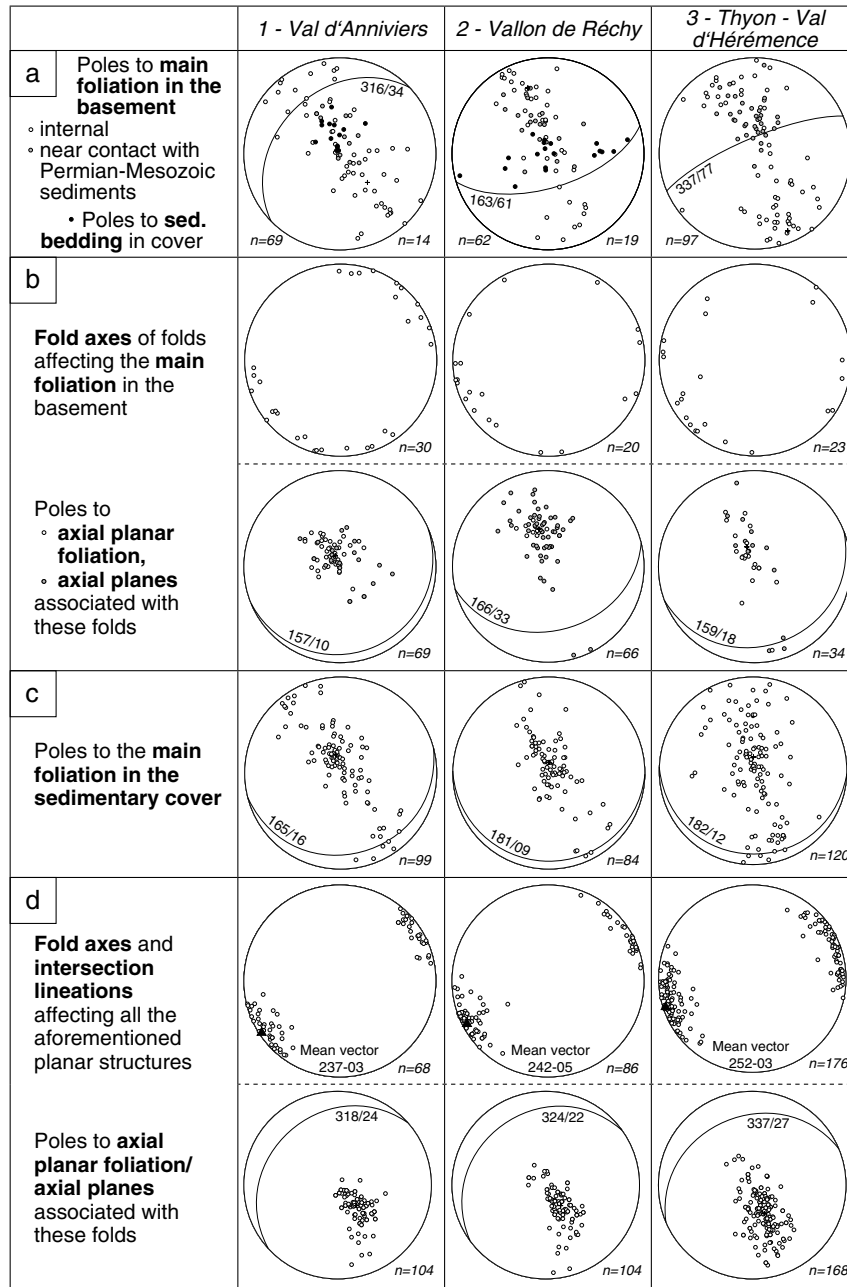


Figure 3. Stereoplots (equal area, lower hemisphere) providing orientations of penetrative structures for the three sectors of Figure 1. Great circles indicate calculated mean orientation of planes, black triangles indicate mean vectors of fold axes. (a) Orientations of the main planar fabric in the basement and the bedding in the sediments. The main foliation in the crystalline basement is often steeply north and south dipping (internal measurements). There is a trend to a shallower orientation in proximity to the upper and lower contact to Permo-Mesozoic sediments (maximum 50 m away from the contact zone). The mean planes were calculated for the foliations from the internal basement only. Note that the mean orientation of the main foliation in the basement of sector 1 (Val d'Anniviers) is north dipping, which is opposite to the general dip of the basement-cover contacts. (b) Fold axis orientations and associated axial planes and axial planar foliations of the main foliation in the basement. Axial planes generally dip toward the south. (c) Orientation of the main foliation in the cover. This foliation is generally slightly south dipping and has a similar orientation to the axial planes and axial planar foliations from the basement shown in Figure 3b. (d) Fold axes, intersection lineations, axial planes, and axial planar foliations from folds, which overprint both the main foliation in the basement and the cover. These folds also refold the folds of Figure 3b. The axial planes and axial planar foliations of these folds dip toward the (N)NW. Orientation of these fold axes and associated axial planes are quite homogeneous for all three sectors.

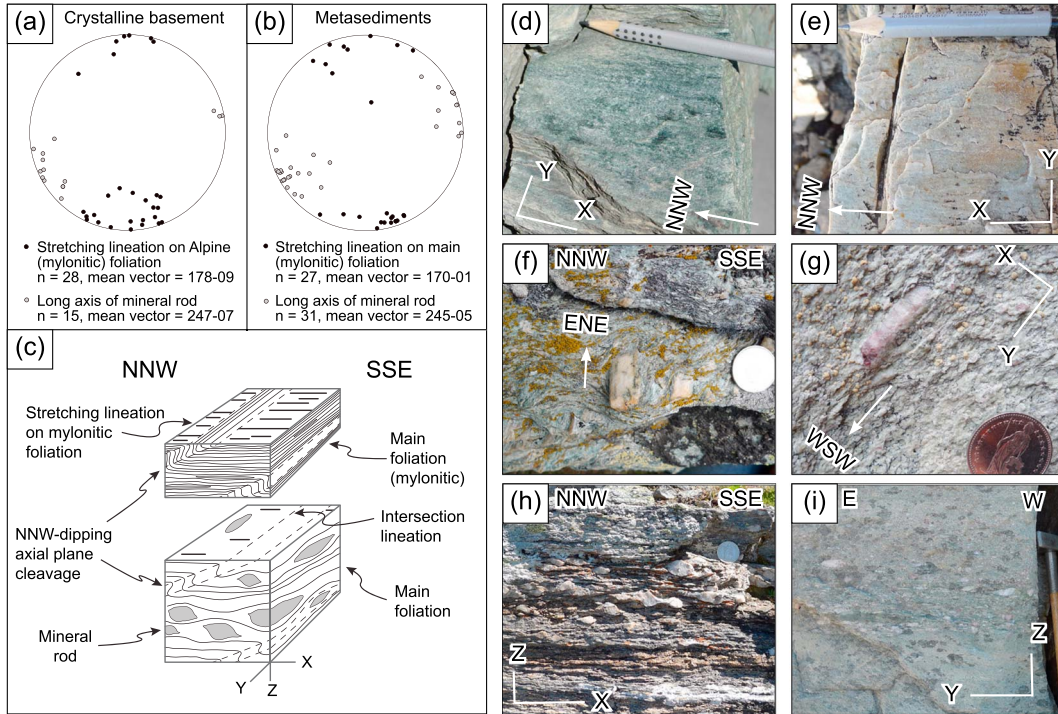


Figure 4. Two types of stretching lineations developed (a) in the crystalline basement and (b) in the metasediments (equal area lower hemisphere projection). (c) Schematic sketch of stretching lineations recorded in highly deformed rocks (above) and moderately deformed rocks (below). Stretching lineations in highly deformed rocks trend N(NW)-S(SE). Moderately deformed rocks often represent L- to LS-tectonites with mineral rods aligned in E(NE)-W(SW) direction. (d) NNW trending stretching lineation in highly deformed micaschist from the basement (612397/118517), pencil for scale. (e) NNW trending stretching lineation in highly deformed quartzite (616671/115573), pencil for scale. (f) ENE-WSW trending quartz rod in moderately deformed Permian metasediment (616717/120622), coin for scale. (g) ENE-WSW trending quartz rod in moderately deformed quartzite (616431/114469), coin for scale. (h) Asymmetric quartz clasts in highly deformed Permian metasediment showing top-to-the-NNW shear sense. The same clasts are symmetrically stretched in ENE-WSW direction (606881/118101), coin for scale. (i) E-W elongated quartz clasts in moderately deformed quartzites. These clasts are less stretched in N-S direction (604962/113558), hammer for scale.

3.1.2. Cover

[28] Within the Permo-Mesozoic sedimentary units present in all three sectors, lithological bedding is generally recognizable and flat lying (Figure 3c). This primary foliation is overprinted by a penetrative, tectonic foliation, which is subparallel or slightly steeper south dipping than the sedimentary layering and lithological contacts (Figures 2e and 3c). The tectonic foliation in the sediments is in most instances subparallel to the SSE dipping axial planes and crenulation cleavage within the basement but scatters more widely (Figures 3b and 3c). N-S trending stretching lineations are preserved on foliation planes and show top-to-the-N shear senses (Figures 4b and 4e). In some cases, bedding planes are isoclinally folded with an axial planar cleavage corresponding to this main foliation.

[29] The scatter in the orientation of the main foliation (Figure 3c) is the result of a later deformational overprint, characterized by mainly south-vergent folds with (E)NE-(W) SW trending fold axes (Figures 2f–2h and 3d). Depending on location and lithology, an axial planar cleavage developed in these south verging folds (e.g., Figure 2g). Both cleavage and axial planes dip mostly to the (N)NW (Figure 3d). The intensity of this second deformation phase increases both toward

the upper limit of the Bernard nappe complex and toward the south.

[30] Similar to porphyroblasts in orthogneisses from the basement, Permian metaconglomerates and conglomerates of the basal quartzites show clasts elongated in a (E)NE-(W) SW direction, perpendicular to the stretching lineation developed on the main tectonic foliation (Figures 4b, 4c, and 4f–4i). Again, no shear sense indicators parallel to this elongation direction are developed, and it is difficult to deduce during which phase these elongated mineral rods formed.

3.2. Structural Variations Along and Across Strike

[31] Apart from the penetrative structures, which are present in the entire study area, the internal structure of the Bernard nappe complex is characterized by significant changes along and across strike. The important variations and characteristics of each sector are therefore described for each sector in more detail.

3.2.1. Sector 1—Val d' Anniviers

[32] This easternmost sector covers the region east of Val d' Anniviers (Figure 1c). This region is dominated by pre-Triassic crystalline basement rocks and Permo-Triassic quartzites, locally with overlying carbonates (Figures 1c and 5a).

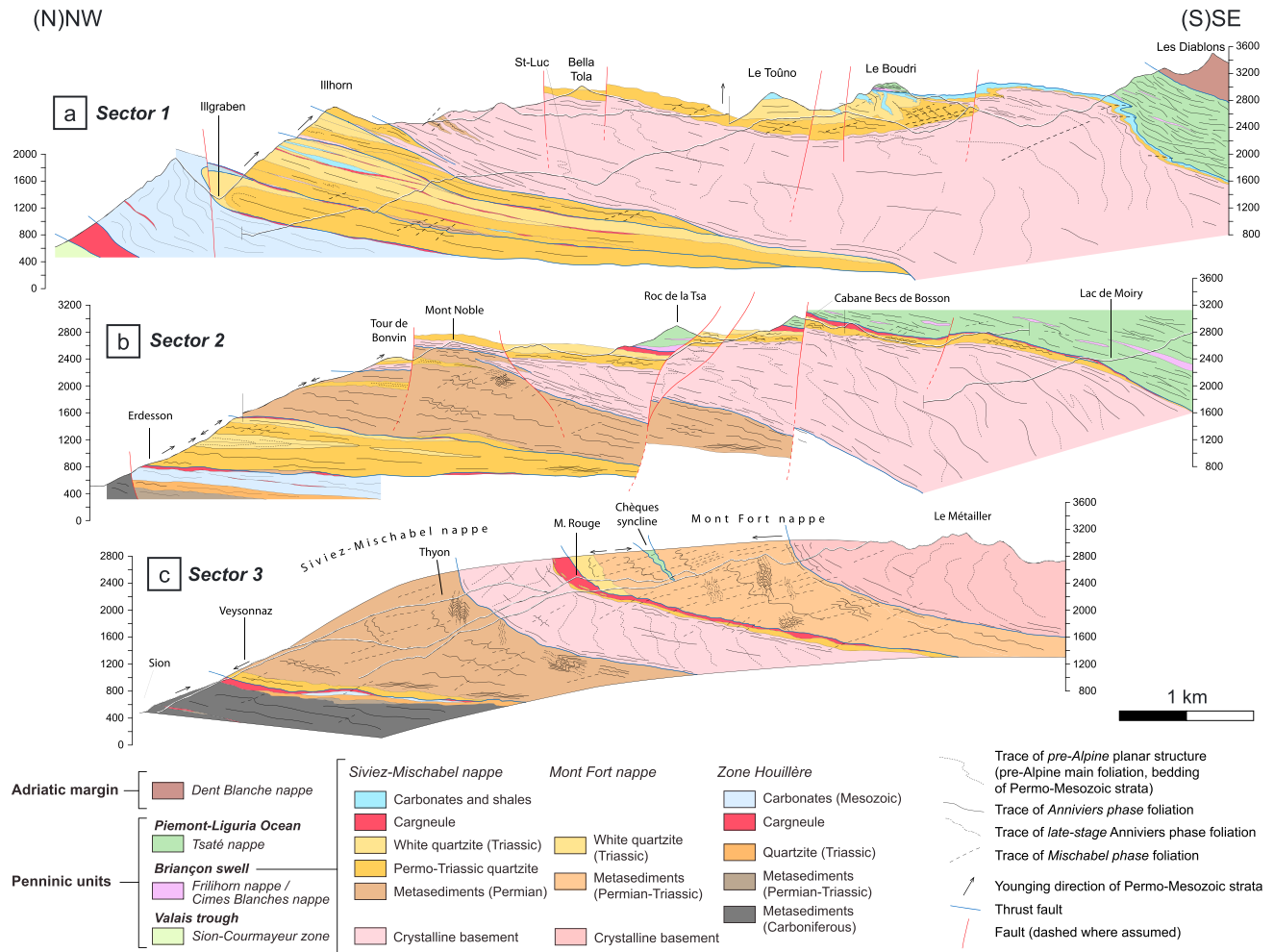


Figure 5. Structural profiles through the three investigated sectors. The profiles are based on the compiled map (Figure 1c) and field observations. The section traces are shown in Figure 1 and are continuous where shown in the profiles and dotted where not shown in the profiles but used for construction. (a) Section 1 is characterized by a massive succession of quartzites in the north and an open backfold, accompanied by a complex top-to-the-south shear zone, in the south. (b) Section 2 shows a complexly folded Permo-Triassic sequence, which is overthrust by a relatively thin frontal basement slice. (c) In section 3, the Mont Fort nappe tectonically overlies the Siviez-Mischabel nappe. The whole nappe pile is openly backfolded. Permo-Triassic metasediments are inverted where directly overlying the Zone Houillère.

Older Permian metasediments are nearly completely absent in this sector. The Permo-Triassic quartzites occur as a basal greenish and an overlying whitish (“Tafelquarzit”) variety. The sedimentary units are exposed in two areas: (1) beneath the main basement unit in the northern part of the sector and (2) above the main basement unit further south (Figures 1c and 5a). A connection between these two areas is nowhere exposed. In the following, we discuss the structure of these two areas separately, since they are important for the large-scale structural geometry of the entire region.

[33] In the northern part of sector 1, below the main basement unit, an up to at least 1800 m thick succession of Permo-Triassic sediments is exposed. This can be best observed from a point with Swiss grid coordinates 612333/124495, which provides insight into a steep and freshly eroded bedrock-section bordering the catchment area of the Illgraben (Figure 5a). The area is crucial for the solution of the “Siviez-Mischabel” dilemma, which states that these rocks are either completely

overturned in the lower limb of a large-scale isoclinal fold or represent a stacked thrust complex. Packages of basal and white quartzites interleaved with cargneule, discontinuous carbonate horizons, Permian conglomerates, and rarely crystalline basement slices build up this massive slope (Figures 1c and 5a). Unraveling the stratigraphic and structural relationships between the different lithologies in this large succession is complex. Our field observations, however, indicate that the succession consists of several stratigraphically upright packages of basal and white quartzites (Figure 5a) separated by zones where the different lithologies are irregularly intercalated. For example, near Chandolin (Figure 1c), an up to 100 m thick sliver composed of cargneule, limestone, and dolomite can be mapped (“Dolomitzug von Chandolin” after Jäckli [1950]). Its lower contact to white quartzite is marked by cargneule, which contains blocks of carbonate and quartzite. The base of the overlying limestone is characterized by several intercalated layers of quartzite (Figure 6a). While the limestone

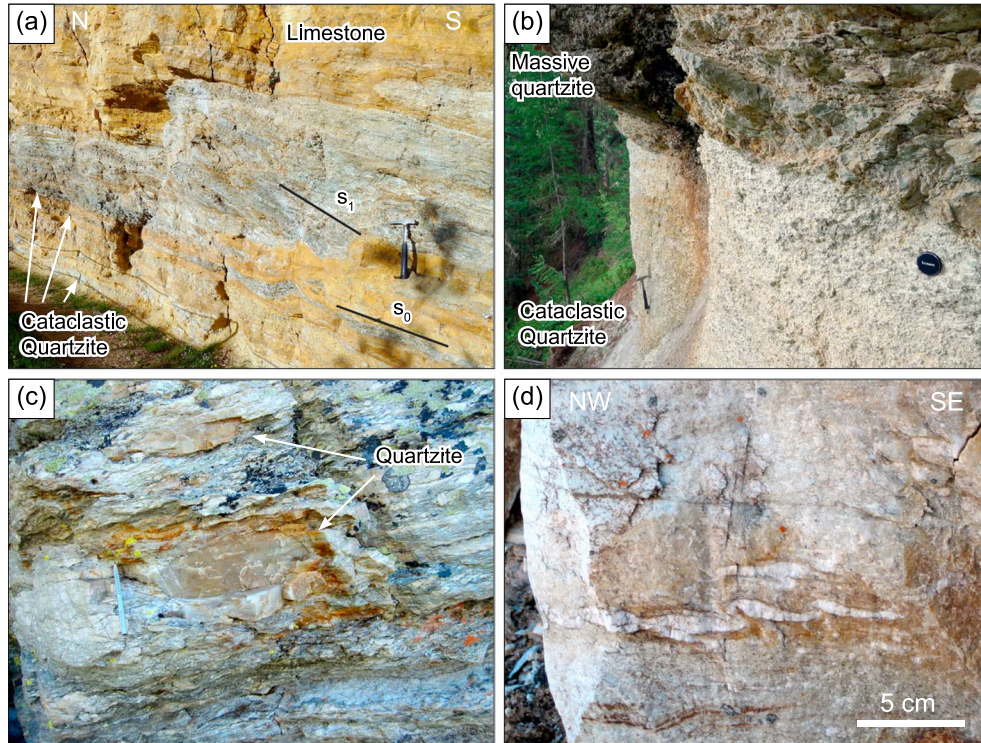


Figure 6. Structural features from the frontal part of sector 1. (a) Limestones and interlayered cataclastic quartzite beds (611416/122546), hammer for scale. (b) Layered cataclastic quartzite, sharply bordered by massive quartzite (611821/122701), lens cover and hammer for scale. (c) Fragments of quartzite embedded into orthogneiss (614861/123234), pencil for scale. (d) Folded quartz vein (631021/123994).

shows a mylonitic foliation, the quartzite is fragmented and gritty and represents a cataclasite (known as “Zuckerquarzit”). The upper contact of the sliver to the overlying quartzite is, again, marked by a several meter thick layer of cataclastic quartzite (Figure 6b). Discontinuous orthogneiss slices also contain angular fragments of quartzite (Figure 6c) and are bordered by cataclastic quartzite. These horizons of cataclastic quartzite occur predominantly within the white quartzite and are mostly subparallel to the lithological contacts and discontinuous in extent. They are best exposed in the frontal part of sector 1, but similar horizons occur throughout the study area within the quartzites and bordering cagneule, carbonates, and/or orthogneisses.

[34] In addition to the cataclastic layers, minor folding of the sedimentary rocks was observed, and two types of folds occur: (1) north-vergent, outcrop-scale folds with the main foliation as axial plane foliation (Figure 6d). These folds are north-vergent independent of their position within the lithostratigraphic sequence; classical s-, m-, and z-geometries indicative for a large-scale isoclinal fold were not observed. (2) The main foliation is very locally folded on a small scale around NE-SW trending fold axes. These folds are SE-vergent with axial planes dipping toward the NW (Figures 3d and 5a).

[35] In summary, the observations of dominantly upright sedimentary sequences interlayered by basement rocks and cataclastic quartzitic horizons and folded into outcrop-scale north-vergent folds point to mainly thrust-related stacking of the entire package in the northern part of sector 1.

[36] In the southern part of sector 1, above the main basement unit, Permo-Mesozoic cover, including carbonates (i.e.,

at Bella Tola and Toûno, Figures 1c and 5a), still rests in an upright and parautochthonous position with respect to the basement. No evaporites occur between the Permo-Triassic quartzites and the younger carbonates. This cover dramatically thins toward the south, above an open basement antiform (Figure 5a). The most interesting area of this upper cover sequence is the Le Boudri area (Figures 5a and 7). Here, the Permo-Mesozoic quartzites and carbonates are isoclinally folded into north facing synclines and anticlines. Phyllitic calcschists occur in some of the cores of the synclines (Figure 7a). In several previous studies this series is interpreted as a condensed stratigraphic sequence from Triassic quartzites to Eocene “wildflysch” [Masson *et al.*, 1980; Marthaler, 1984; Sartori, 1987a]. However, there is no unambiguous evidence for the existence of Eocene rocks within this sequence [Marthaler *et al.*, 2008b], and the contact between the carbonates and the calcschists is very sheared (Figure 7a). We therefore interpret the entire calcschist package including the prasinites higher up in the sequence as part of the Tsaté nappe. Southeast of Le Boudri, a discontinuous basement slice occurs within the quartzite and constitutes the core of an anticline (Figure 5a). Measured fold axes are NE-SW trending in this area, and a well-developed, originally subhorizontal to south dipping axial planar foliation is associated with these folds. These isoclinal folds are strongly overprinted by subsequent south directed shearing and backfolding. The main foliation is crenulated and backfolded with an enveloping surface steeply south and even north dipping (Figures 5a and 7a). The axial planar cleavage associated with these south-vergent folds generally dips toward the

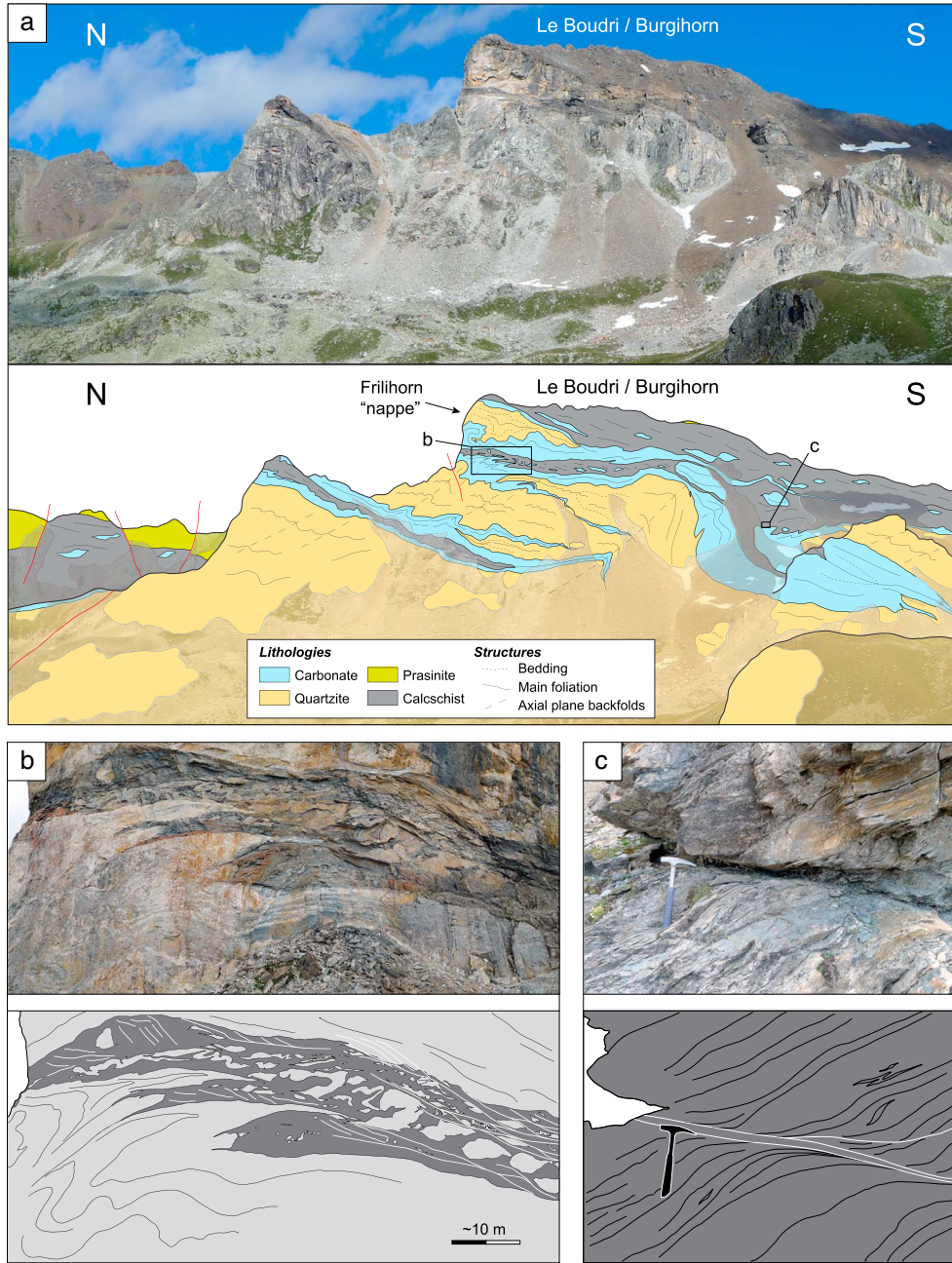


Figure 7. Field observations from sector 1. (a) Photograph and geological interpretation of the Le Boudri area (Toûno klippe, Figure 1c) viewed from the west. Quartzites and carbonates of the Siviez-Mischabel nappe are overlain by and complexly folded with calcschists and prasinites of the Tsaté nappe. Early isoclinal north-vergent folds are reoriented by younger south-vergent folds, which are accompanied by top-to-the-south shear bands. The uppermost complexly deformed south facing fold structure with quartzites in the core was traditionally ascribed to the Frilhorn nappe [e.g., *Marthaler et al.*, 2008a]. (b) The footwall carbonates are folded into south-vergent isoclinal folds, and detached fragments of carbonates are incorporated into a (C'-type) shearband network of calcschists (note the scale!). (c) Example of a C'-type shear band cross-cutting Tsaté calcschists indicating a top-to-the-south shear sense (616752/ 115546), hammer for scale. Figures 7b and 7c are details from Figure 7a.

NW (Figures 2g–2h). However, approaching the overlying Tsaté nappe, the axial planes are no longer NW dipping but horizontal or even south to SE dipping (Figure 5a).

[37] Above these, isoclinally folded and back-sheared parautochthonous carbonates follow a rather flat-lying zone mainly composed of phyllitic calcschists (Figure 7a). Within

these calcschists, blocks of carbonates (both limestone and dolomite), which commonly have an orange to brownish patina, quartzites, and, in higher levels, prasinites occur. Deformation in this mélangé zone is highly complex. Networks of shear bands showing top-to-the-S movement cut across the mélangé zone (Figure 7). The carbonates

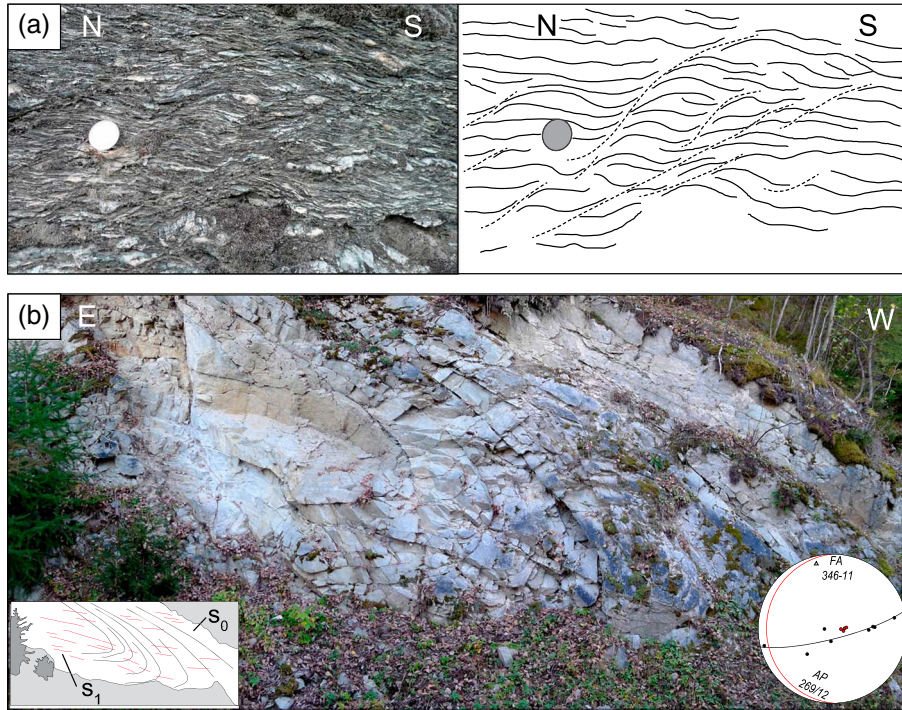


Figure 8. Field observations from sector 2. (a) Shear bands indicating a top-to-the-north movement observed in Permo-Triassic conglomerates at the base of the Siviez-Mischabel nappe (599052/ 114241), coin for scale. (b) Folded white quartzite in the northern part of sector 2 (603397/ 121124), trees for scale. Poles to bedding planes lie on a great circle and define a fold axis (FA), which plunges to the north, and the associated constructed axial plane cleavage (AP) dips gently toward the west.

beneath are folded into south facing folds showing a transition to completely disrupted fragments of carbonates, which are incorporated into the shear zones and are internally multiply folded (Figure 7b). Locally it is possible to observe sheath folds with axes parallel to the stretching lineation; they are indicative of high strain parallel to the regional south directed transport direction. In the same area, distinct shear bands indicating top-to-the-south movement cut through the carbonates and detach several decameter-sized blocks of competent lithologies (Figures 7a–7c). Above this mélangé zone, the headwall making up the steep north and west faces of Le Boudri contains a recumbent south facing anticline with quartzite in its core (Figure 7a). This structure, previously ascribed to the Frilihorn nappe [Marthaler *et al.*, 2008a], conspicuously resembles the smaller isoclinal folds within the mélangé zone and could represent an anticline detached by a top-to-the-S shear zone.

[38] These observations show that the south-vergent folds with NW dipping axial plane, which are present throughout the study area, are accompanied by top-to-the-south shearing near the upper limits of the Siviez-Mischabel nappe. This shearing detached parts of the parautochthonous sedimentary cover of the Siviez-Mischabel nappe and incorporated blocks and lenses of carbonate and quartzites (ascribed to the Frilihorn nappe) into the overlying Tsaté nappe.

3.2.2. Sector 2—Vallon de Réchy

[39] The central sector covers the area around and SSE of Vallon de Réchy (Figure 1c). As in sector 1, this sector contains a northward thinning central basement unit, which separates a lower from an upper metasedimentary unit (Figure 5b). However, in contrast to sector 1, the lower sedimentary unit

contains a thick sequence of Permian metasediments. These Permian metasediments are only present below the basement unit and not above. The two contacts between the crystalline basement and Permo-Mesozoic cover units are different: the lower contact of the basement with the Permian metasediments corresponds to a mylonitic high-strain zone with north trending lineation and top-to-the-N shear sense, branching out in its frontal part. The upper contact of the basement with the Permo-Triassic quartzites is less sheared (Figure 5b).

[40] Unraveling the structure of the lower metasedimentary unit is more complex. The main body of Permian metasediments is dominated by a main, slightly south dipping foliation, overprinted by south-vergent folds with north dipping axial planes (Figures 3d and 5b). No folds associated with the main foliation were observed. The Permian metasediments contain small layers of quartzite at different levels (Figure 5b). No folds are observed within these quartzite layers. Below the main body of Permian metasediments, an up to 800 m thick succession of quartzites separates the Permian metasediments from the underlying cagneule and carbonates of the Zone Houillère (Figure 5b). The contact zone between the quartzites and the Permian metasediments is locally marked by cagneule interfingering with the quartzites (Figure 5b), and top-to-the-north shear bands are dominant in the lower part of the Permian metasediments (Figure 8a). Within the quartzites, a mesoscale isoclinal fold structure can be observed (Figure 8b). This fold has a north trending fold axis (Figure 8b), which is parallel to the stretching lineation observed in the Permian metasediments. In the eastern part of sector 2, the lower quartzites are again underlain by a package of Permian metasediments (Figure 1c).

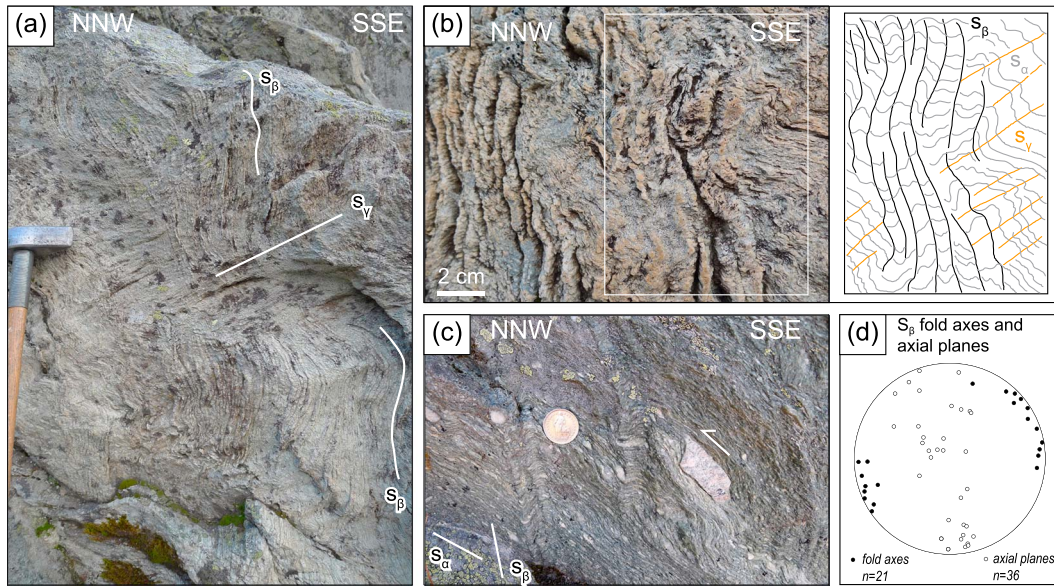


Figure 9. Field observations from sector 3. In this sector, there are locally three overprinting foliations. The main foliation (S_α) is overprinted by a spaced crenulation cleavage (S_β), which is again overprinted by another spaced crenulation cleavage (S_γ). Location of Figures 9a and 9b is (593320/109069). (c) Kinematics during the development of the main foliation (S_α) is top-to-the-NNW, the angle between S_α and S_β is around 40° (594492/114033), coin for scale. The S_β crenulation indicates NNW-vergent folding. (d) Fold axes associated with S_β crenulation trend ENE-WSW.

[41] As in sector 1, the upper parautochthonous metasedimentary cover wedges out toward the SE (Figure 5b). No carbonate is preserved on top of the quartzite in this sector, and the quartzites are overlain by cargneule (Figure 5b). However, relict carbonates of the Mont Fort cover are preserved in the southwestern part of sector 2 (near Evolène, Figure 1c). Similar to sector 1, the overlying Tsaté nappe hosts a range of carbonaceous units ascribed to the Cimes Blanches nappe [e.g., Steck *et al.*, 1999; Sartori and Epard, 2011]. South-vergent folds affecting the main foliation occur all over the sector but are more pervasive in the upper and southern parts of the units. In the Tsaté nappe, the south-vergent folds are accompanied by top-to-the-S shear bands. Units attributed to the Cimes Blanches nappe are commonly fragmented and show complex deformation patterns. The folds and shear bands indicate that, similar as in sector 1, the upper part of the Siviez-Mischabel nappe in sector 2 and the overlying units were affected by top-to-the-south shearing.

3.2.3. Sector 3—Thyon Val d'Hérémece

[42] The westernmost sector covers the ridge between Val d'Hérens and Val de Nendaz (Figure 1c). In this sector, the Mont Fort nappe is thrust on top of the Siviez-Mischabel nappe (Figures 1b, 1c, and 5c). The tectonic contact between the two units is marked by a prominent cargneule layer (Figure 5c). Both nappes contain large bodies of mainly Permian metasediments, which are overlain by crystalline basement. The upper parautochthonous sedimentary cover of the Siviez-Mischabel nappe is poorly expressed by relics of basal quartzite, and the one of the Mont Fort nappe is generally lacking. Characteristic for this sector is the open large-scale backfold, which affected both nappes (Figure 5c).

[43] As in sector 2, the structure of the large mass of Permian metasediments within the Siviez-Mischabel nappe is complex. At the base of the large package, Permian conglomerates

continuously grade into finer-grained basal quartzite (see also Sartori and Epard [2011]), indicating an inverse stratigraphic succession for these sediments (Figures 1c and 5c). This can be best observed east of Hérémece (between sectors 2 and 3, 599075/1174235) and northwest of Veysonnaz (591825/115620). In these places shear bands indicating a top-to-the-NNW movement similar to the ones in sector 2 occur (Figure 8a).

[44] The large package of metasediments of the Mont Fort nappe contains both Permian metasediments and quartzitic microconglomerates, which cannot be differentiated at the map and profile scale (Figures 1c and 5c). White quartzite is present in the northernmost part of this package and, similar to the Siviez-Mischabel nappe below, points to an inverted succession at the base of the nappe. In addition, a complex fold structure occurs within this package: At the eastern termination of the Mont Fort nappe (near Evolène, Figure 1c) relics of Mesozoic carbonates are folded with quartzite and Permian metasediments, and a thin sliver of the Tsaté nappe reaches far into the Mont Fort metasediments (Figures 1c and 5c). This indicates that the thrust contact between Tsaté and Mont Fort nappes is isoclinally folded, forming a large-scale synform in sector 3, and an antiform near Evolène (Figures 1c and 5c) (“Chèques syncline” and “Evolène anticline” after Allmann, [1987] and Sartori *et al.* [2006]). The axial plane foliation of these large-scale folds corresponds to the main foliation in rocks of both nappes.

[45] Finally, a last important observation in sector 3 is the local occurrence of three overprinting foliations (Figures 5c and 9). In the Permian to Triassic metasediments, the main foliation (S_α in Figure 9) is locally overprinted by a spaced, asymmetric crenulation cleavage (S_β). This cleavage dips about 40° steeper to the SSE than the main foliation and indicates NNW-vergent folding around ENE-WSW trending

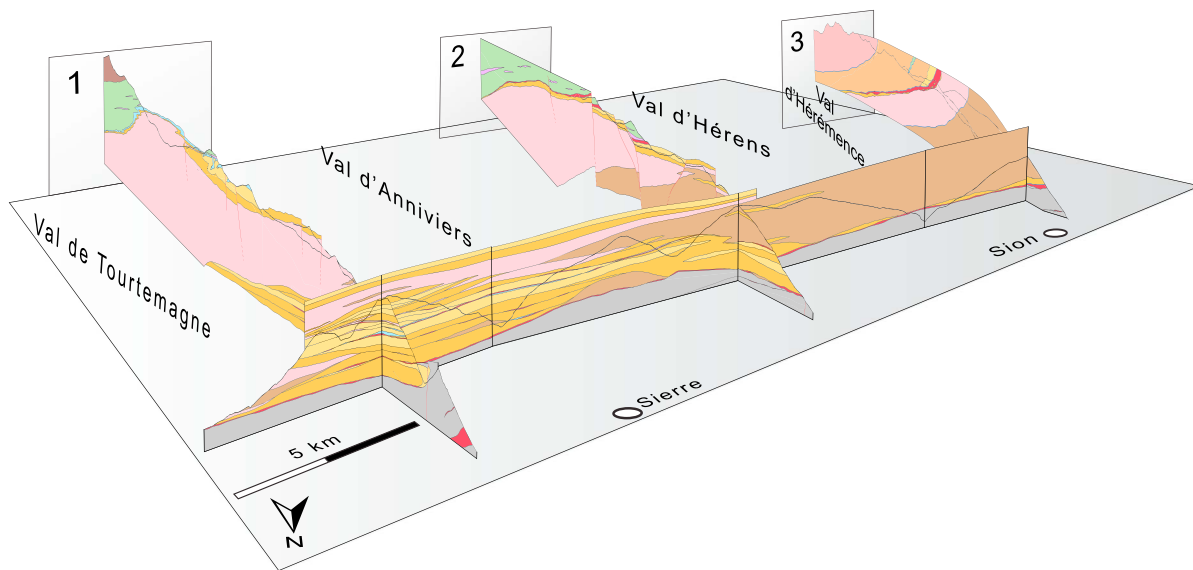


Figure 10. Three-dimensional sketch of the study area viewed toward the SSW. There is a tremendous lithological change from ENE to WSW in the frontal part of the Siviez-Mischabel nappe. While the NE part of the study area is characterized by a nappe pile, mainly composed of Permo-Triassic quartzites, the western part is dominated by Permian metasediments. The transition zone (sector 2) shows complex isoclinal recumbent folds. Tectonic units below the Siviez-Mischabel nappe are gray-colored; color-coding of the other units is identical to the one used in Figures 1c and 5. Cross-sectional traces are given in Figure 1c.

fold axes (Figure 9d). This cleavage is in its turn reoriented by coaxial folds with axial planes dipping toward the NNW (S_{γ} in Figure 9; Figure 3d).

3.3. Summary of 3-D Architecture and Finite Geometry

[46] Figure 10 schematically displays and summarizes the 3-D architecture of the central Bernard nappe complex. Extrapolation outside of our study area remains speculative. From this figure, one can deduce the following important large-scale east-west variations in structural architecture: (1) There is a dramatic E-W change in lithology and structure from the predominantly normal-lying sequence of Permo-Triassic quartzites underlying crystalline basement in sector 1 to the partly inverted Permian metasediments underlying the crystalline basement of sector 3 (Figures 5 and 10). Along the transition zone (sector 2), quartzites indicate recumbent folds with complex 3-D geometries (Figures 5b and 8b). (2) The basement unit of the Siviez-Mischabel nappe continuously thins from sector 1 to sector 3. (3) The Mont Fort nappe is absent in sector 1 and appears just west of sector 2, where it is complexly folded with rocks of the Tsaté nappe. (4) While only a slight updoming is registered in the southern part of sector 1, the entire nappe pile is backfolded on a large scale in sector 3 (Figure 10). (5) The major top-to-the-south shearing observed in the upper part of the Siviez-Mischabel nappe in sector 1 continuously decreases in intensity toward the west and is nearly absent in sector 3.

4. Interpretation and Deformation History

[47] Based on our field observations, we charted our results in a tectonic sequence diagram (Figure 11), which allows unprejudiced correlation of all structures over space (sectors), geological units (lithologies), and time [Forster and Lister,

2008]. This allowed us to deduce a sequence of six Alpine deformation phases (D1 to D6) from the observed structural relationships. Three of these deformation phases are mainly responsible for today's geometry of the Bernard nappe complex and were therefore given names: the Evolène and Anniviers phases (introduced here) and the Mischabel phase (following Milnes *et al.* [1981]).

4.1. Pre-Alpine Structures

[48] The main foliation in all basement units primarily reflects pre-Alpine deformation and most likely formed during the Variscan orogeny. This interpretation is based on two arguments. First, white mica ages defining the dominant foliation in the basement yield Permo-Carboniferous ages [Soom, 1990; Markley *et al.*, 1998]. Second, the generally steep dipping main foliation in the crystalline basement has a clearly different orientation from the main Alpine (generally flat lying to gently south dipping) foliation in the sedimentary units.

4.2. D1 (Evolène Phase)

[49] The fact that the thrust contact between the Tsaté nappe and the Bernard nappe complex is isoclinally folded (e.g., “Chèques syncline”, Figure 5c) points to an early phase of detachment and thrusting during the Alpine orogenic cycle. The Klippen and Breccia nappes were detached from their substratum, probably along major evaporite horizons overlying Permo-Triassic quartzites. However, locally Permo-Triassic and younger strata of the Briançon cover remained on the basement (Barrhorn and Toûno series), possibly as a result of a Jurassic graben structure (as suggested by Sartori [1987b]) or simply due to the lack of a Triassic detachment horizon in this area [e.g., Sartori *et al.*, 2006]. The Tsaté nappe was emplaced on top of the Bernard nappe

		Tectonic Sequence							Time	
Val d'Anniviers	younger sediments	Ssed	Smain mostly parallel to Ssed	Fiso recumbent variable fa ap S-dipping			Fopen - tight ENE-WSW fa SSE-vergent ap NW-dipping	SZ in the S / at the top S-dipping top S	HAF	
	Triassic-Permian quartzites	Ssed	Smain mostly parallel to Ssed	Fiso recumbent variable fa ap S-dipping	Lmin N-S Lrod ENE-WSW		Scr NW-dipping Fopen - tight ENE-WSW fa SSE-vergent ap NW-dipping		Ssemibrittle subvertical S-side up HAF	
	Permian meta-sediments	Ssed	Smain mostly parallel to Ssed	Fiso-open recumbent variable fa ap S-dipping	Lmin N-S Lrod ENE-WSW		Scr NW-dipping Fopen - tight ENE-WSW fa SSE-vergent ap NW-dipping		HAF	
	Crystalline basement	Spre-Alpine subvertical	SZ top N subhorizontal - basal - intra-crystalline - contact to cover	Fiso-open recumbent variable fa ap S-dipping	Lmin N-S		Fopen - tight ENE-WSW fa SSE-vergent ap NW-dipping		HAF	
Vallon de Réchy	younger sediments	Ssed	Detachment / cover substitution	Fiso recumbent variable fa ap S-dipping			Fopen - tight ENE-WSW fa SSE-vergent ap NW-dipping	SZ in the S / at the top S-dipping top S		
	Triassic-Permian quartzites	Ssed	Smain mostly parallel to Ssed	Fiso recumbent variable fa ap S-dipping	Lmin N-S Lrod ENE-WSW		Scr NW-dipping Fopen - tight ENE-WSW fa SSE-vergent ap NW-dipping	SZ in the N / at the base subhorizontal top N	Ssemibrittle subvertical S-side up HAF	
	Permian meta-sediments	Ssed	Smain mostly parallel to Ssed	Fiso recumbent variable fa ap S-dipping	Lmin N-S Lrod ENE-WSW	Fopen - tight ENE-WSW fa NNW-vergent	Scr S-dipping	Scr NW-dipping Fopen - tight ENE-WSW fa SSE-vergent ap NW-dipping	SZ in the N / at the base subhorizontal top N	Ssemibrittle subvertical S-side up HAF
	Crystalline basement	Spre-Alpine subvertical	SZ top N subhorizontal - basal - intra-crystalline - contact to cover	Fiso-open recumbent variable fa ap S-dipping	Lmin N-S		Fopen - tight ENE-WSW fa SSE-vergent ap NW-dipping		HAF	
Thyon - Val d'Hérémence	younger sediments	Ssed	Detachment / cover substitution	Fiso recumbent variable fa ap S-dipping			Scr NW-dipping Fopen - tight ENE-WSW fa SSE-vergent ap NW-dipping			
	Triassic-Permian quartzites	Ssed	Smain mostly parallel to Ssed	Fiso recumbent variable fa ap S-dipping	Lmin N-S Lrod ENE-WSW	Fopen - tight ENE-WSW fa NNW-vergent	Scr S-dipping	Scr NW-dipping Fopen - tight ENE-WSW fa SSE-vergent ap NW-dipping	SZ in the N / at the base subhorizontal top N	Ssemibrittle subvertical S-side up HAF
	Permian meta-sediments	Ssed	Smain mostly parallel to Ssed	Fiso recumbent variable fa ap S-dipping	Lmin N-S Lrod ENE-WSW	Fopen - tight ENE-WSW fa NNW-vergent	Scr S-dipping	Scr NW-dipping Fopen - tight ENE-WSW fa SSE-vergent ap NW-dipping	SZ in the N / at the base subhorizontal top N	Ssemibrittle subvertical S-side up HAF
	Crystalline basement	Spre-Alpine subvertical	SZ top N subhorizontal - basal - intra-crystalline - contact to cover	Fiso-open recumbent variable fa ap S-dipping	Lmin N-S		Fopen - tight ENE-WSW fa SSE-vergent ap NW-dipping		HAF	
			"Anniviers phase"			"Mischabel phase"				
		D1	D2		D3		D4		D5	D6

Figure 11. Tectonic sequence diagram after *Forster and Lister* [2008]. The different fabrics observed in each lithological unit of each sector are correlated, and a regional tectonic scheme (D1–D6) is inferred. S denotes planar fabrics with the following subscript: pre-Alpine = pre-Alpine fabric, sed = sedimentary bedding, main = main Alpine foliation, cr = crenulation cleavage, semibrittle = semibrittle cleavage. In addition, orientations of planar structures are given. F indicates observed folding phase, with the corresponding geometrical description in subscript (shape of folds, fold vergence, orientation of fold axes (fa), and associated axial planes (ap)). L refers to observed lineation, with min = mineral stretching lineation on main foliation planes, rod = long axis of mineral/pebble rod, and the orientation of each lineation indicated. SZ denotes observed shear zone, with orientation and shear sense indicated. HAF stands for high angle (close to vertical) brittle fault. Dashed line between fabric elements indicate that they probably formed simultaneously. Gray background highlights penetrative fabrics. D indicates deduced deformation phases. D1 corresponds to the “Evolène phase” in the text.

complex, which is a classic example of cover substitution [e.g., *Escher et al.*, 1993; *Sartori and Marthaler*, 1994]. In addition, the Permo-Triassic quartzites of the frontal Briançon domain in the eastern study area were probably already stacked along brittle thrusts during this phase. In the western study area, the presence of a large graben filled with Permian sediments probably inhibited the formation of a similar thrust stack. Due to the strong post-Evolène overprint, D1 structures are rarely preserved and have only been observed in small-scale D2 fold hinges and microlithons. Large-scale fold structures related to the Evolène phase were not observed in the study area.

4.3. D2 (Anniviers Phase)

[50] This phase represents the main Alpine deformation in the investigated area. During this phase, slices of Briançon basement detached from their substratum and were mainly

thrust over metasedimentary rocks. In the crystalline basement units, deformation related to this phase is heterogeneously distributed with the strain intensity increasing toward both the lower and upper contacts to Permo-Mesozoic metasedimentary units. The flat-lying to south dipping foliation with north trending stretching lineations and mainly WSW-ENE trending folds are the result of this deformation phase (Figures 2a–2d, 3b, 4a, and 4d). These features imply a component of vertical shortening coeval with N(NW) directed tectonic transport.

[51] In the Permo-Mesozoic metasediments, imbrication and thrusting, which in the eastern study area may have initiated already during D1, probably continued without a significant change in the orientation of the stress field during D2 and a complexly sheared and intercalated sequence of Permo-Mesozoic lithologies was produced below the basement slices during this phase (Figure 5a). In the western

study area, the Permian metasediments and Permo-Triassic quartzites were partly isoclinally folded during this phase, causing local inversion of the stratigraphy (Figure 5c).

[52] The parautochthonous sedimentary cover of the basement slices, together with rocks of the Tsaté nappe, was affected by isoclinal, north-vergent folding during this phase. In the southern part of sector 1, the crystalline basement is locally incorporated into D2 folding (Figure 5a), but overall D2 folds in the parautochthonous cover may generally be considered as detachment folds (e.g., near Le Boudri in Figure 5a).

4.4. D3 (Late-Stage Anniviers Phase)

[53] The local observation of three overprinting foliations in the western study area (Figure 9) is in our opinion the result of a change in the stress field during a late stage of the Anniviers phase, overprinted by the subsequent Mischabel phase (D4). S_{β} formed in our opinion during the same general north-vergent deformation as S_{α} but locally provoked a remarkable reorientation of S_{α} (Figure 9).

4.5. D4 (Mischabel Phase)

[54] The Mischabel phase affected all lithologies and can be recognized throughout the study area. It is characterized by folds that refold the pre-Alpine and D1 to D3 planar structures and that are mostly associated with a (N)NW dipping crenulation cleavage (Figures 2f–2h, 3d, and 9). These folds are parasitic to (1) the huge backfold of the nappe pile in the west of the study area (Figure 5c), (2) the doming of the Siviez-Mischabel nappe and overlying Combin zone in the east of the study area (Figure 5a), and (3) the large-scale south facing folds at the upper limit of the Bernard nappe complex (Figure 7). Furthermore, these structures are associated with the Mischabel backfold east of the study area [Klein, 1978; Müller, 1983]. Backfolding is a result of top-to-the-south shearing, which localized at the upper limit of the Bernard nappe complex. Thereby parts of the parautochthonous cover were detached and incorporated into the Tsaté nappe (Figure 7).

[55] The fact that Mischabel phase structures are prevalent in the upper and southern parts of the Bernard nappe complex exposed in the study area together with the observation of top-to-the-N(NW) shear bands at the base of the Siviez-Mischabel nappe may indicate that thrusting toward the north along the basal thrust continued during this deformation phase.

4.6. D5 (Vanzone Phase) and D6

[56] Semibrittle to brittle structures are present all over the area. Locally, a spaced subvertical cleavage is present in the Permo-Mesozoic sediments, where quartz deformed in a semibrittle manner. Slickenlines on such planes clearly indicate north block-down movement, but displacements are small (cm-scale). These structures may be correlated with late backfolding and backthrusting along the Insubric line, which is typically expressed by steep planar fabrics (Vanzone phase after Milnes *et al.* [1981]). In addition, brittle faults (D6) intersect basement and cover rocks (Figure 1c), and kinematic indicators point to normal and dextral strike-slip movements. These structures are most probably related to movement along the Simplon-Rhône fault (Figures 1b and 1c) [Mancktelow, 1992; Champagnac *et al.*, 2003].

5. Discussion

5.1. Large-Scale Structure of the Siviez-Mischabel Nappe—Fold Nappe or Thrust Stack?

[57] It has long been a matter of debate whether the Siviez-Mischabel nappe represents a basement-cored fold nappe with a normal and an inverted limb or whether it represents a thrust stack consisting of dominantly right-way-up units [Argand, 1909; Jäckli, 1950; Escher *et al.*, 1988; Markley *et al.*, 1999]. According to our field results, there is no simple answer to this question, and this answer has to be presented in two parts. (1) In the eastern part of the study area, where Permo-Triassic quartzites overlie and underlie crystalline basement rocks, there are according to our observations no convincing indications for a large-scale isoclinal recumbent fold in the sense of, for example, Escher *et al.* [1988]. Normal-lying quartzite packages underlying the main basement unit are strongly imbricated, and the contact to the basement represents a major thrust zone (e.g., Figures 5a and 6), as also proposed by Markley *et al.* [1999]. Therefore, we consider that the Siviez-Mischabel nappe in the eastern part of the study area mainly represents an Alpine thrust stack. (2) The western part of the study area, however, has a clearly different structure. Here, crystalline basement overlies Permian metasediments and is itself overlain by Permo-Triassic quartzites (Figures 5b, 5c, and 10). This lithological asymmetry suggests the presence of a Permian graben structure and argues against a large-scale simple isoclinal fold nappe structure with an upper normal and a lower inverted limb, and moreover field observations indicate the presence of a major thrust at the base of crystalline basement units. Nevertheless, Permo-Triassic metasediments are in an inverted position at the contact with the Zone Houillère, and isoclinal folds occur within these Permo-Triassic sediments (Figures 5b and 5c). These inverted sequences are in our opinion the direct result of the inversion of a graben filled with Permian metasediments [Thélin *et al.*, 1993]. The inversion of the Permian graben during the Anniviers phase resulted in complex isoclinal folding of strata and an overturned limb at the basal front (Figure 5). So even though there are inverted strata in the western part of our study area, this does not necessarily argue for a large-scale fold nappe model for the entire nappe but rather results from complex graben inversion. We therefore suggest that the Siviez-Mischabel nappe should not be considered as a simple large-scale isoclinal basement-cored fold nappe. Imbricate thrusting is a more adequate model to describe its structure. The internal structure is largely controlled by the presence or absence of Permian metasediments.

5.2. How Important Is Top-to-the-West/Southwest Shearing?

[58] An important issue regarding the tectonometamorphic evolution of the Siviez-Mischabel nappe and the entire Bernard nappe complex is the significance of (E)NE-(W)SW trending lineations, which are present all over the study area (Figure 4). According to Steck [1984; 1990; 2008], E(NE)-W(SW) trending stretching lineations occur dominantly in the Simplon area and south of it, diminishing westward along a corridor following the Rhône valley. In this model, they are related to a broad extensional ductile shear zone (Simplon ductile shear zone) that is interpreted to have developed in the Early Oligocene. This is an older shear

zonethan the Simplon Fault Zone in the sense of *Campani et al.* [2010]. *Genier* [2007] reports E(NE)-W(SW) trending stretching lineations especially from the base and the northern frontal part of the Siviez-Mischabel nappe (east of our study area) and also relates the lineations to *Steck's* Simplon ductile shear zone. *Pleuger et al.* [2008] document pre-Mischabel phase, orogen-parallel extension with a top-to-the-SW shear sense in the SW Monte Rosa nappe. Finally, *Sartori et al.* [2006] and *Sartori and Epard* [2011] propose the existence of subhorizontal “postnappe” shear zones at several levels within the Bernard nappe complex. They infer WSW directed shearing and interpret these shear zones to represent similar structures as the Simplon ductile shear zone [e.g., *Steck*, 1990] but predating the latter and also predating the Mischabel phase deformation.

[59] According to our field results, the importance of top-to-the-W/SW shearing within the central Bernard nappe complex is limited for several reasons. (1) The E(NE)-W(SW) trending stretching lineations are mainly represented by elongated mineral rods, which occur between mica-rich Anniviers phase foliation planes (Figures 4f–4i). They are not tied to a newly developed foliation, which could represent a distinct phase of top-to-the-west shearing. (2) We could nowhere observe unequivocal shear sense indicators on any plane parallel to this lineation (Figures 4c and 4i), suggesting that the lineation is not associated with a simple top-to-the-west shear regime. (3) Except for small-scale spaced crenulation cleavage associated with top-to-the-NNW folding (Figure 9), no structures were observed that developed chronologically between the Anniviers phase and the Mischabel phase (Figure 11).

[60] Based on these arguments, we suggest that the E(NE)-W(SW) trending ductile stretching lineations in the central Bernard nappe complex did not form during a distinct deformation phase and that they are not related to a top-to-the-west/southwest simple shearing event. Instead, we suggest that they are the result of strain superposition during the Anniviers and Mischabel phases. Moderately deformed rocks within the Bernard nappe complex, i.e., rocks away from high-strain zones, accommodated a component of orogen-parallel stretching during ductile deformation. Both Anniviers and Mischabel phases are characterized by noncoaxial general shear deformation involving flattening perpendicular to the foliation planes and stretching perpendicular to the direction of shear (i.e., orogen-parallel stretching in a W-E/SW-NE direction). These stretching lineations represent a finite strain state and not a distinct top-to-the-west/southwest shearing event.

5.3. The Nature of the Frilhorn and Cimes Blanches Nappes: Importance of Top-to-the-South Shearing

[61] A third debated topic in our study area is the nature and origin of the Frilhorn and Cimes Blanches nappes (Figure 1c). Both their tectonic position and their paleogeographic origin is still controversial. In the model of, for example, *Froitzheim et al.* [2006] and *Pleuger et al.* [2007], the Cimes Blanches and Frilhorn nappes are derived from the sedimentary cover of the Dent Blanche-Sesia unit. In this model, they were emplaced northward along a major thrust zone on top of the Bernard nappe complex and were themselves overthrust by the Tsaté nappe. However, the internal stratigraphy of the Frilhorn and Cimes Blanches nappes resembles strongly the stratigraphy of typical Briançonnais

cover. Therefore, *Marthaler et al.* [2008b] suggest that the Cimes Blanches and Frilhorn nappes originate from the Briançon continental margin and represent possibly olistoliths, which slid southward into the S-Penninic oceanic basin during opening of this basin. Subsequently, the development of an accretionary prism during subduction led to the incorporation of these margin sediments into a “tectono-sedimentary mélange zone” together with rocks of the Tsaté nappe.

[62] Our field observations from the southern sector 1, where the Frilhorn nappe is exposed, support the model of Briançon derivation [*Marthaler et al.*, 2008b] but suggest a different mechanism for emplacement of these rocks. As shown in Figure 7, the blocks and lenses ascribed to the Frilhorn nappe represent detached units of the parautochthonous cover of the Siviez-Mischabel nappe, which were sheared off from their substratum during Mischabel phase top-to-the-south shearing and backfolding. So instead of pre-Alpine olistolithic southward emplacement, we suggest postnappe southward shearing as the mechanism for emplacement of these blocks. Given this interpretation, the term “nappe” is rather misleading, since these units do not constitute proper Alpine nappes emplaced during northward thrusting, as implied in the model of *Froitzheim et al.* [2006] and *Pleuger et al.* [2007], but represent units detached from the footwall during Mischabel phase south directed shearing.

[63] Our interpretation is mainly based on observations concerning the Frilhorn nappe in the southern part of sector 1 (Figure 7), but we made similar observations for slices of the Cimes Blanches nappe in sector 2 (Figure 1c). Whether our new interpretation is also valid for the rest of the Cimes Blanches nappe needs to be verified by further studies. Its validity is problematic in the southwest of our study area, because there is no obvious source for units attributed to the Cimes Blanches nappe. However, carbonate relicts of the Mont Fort cover occur near Evolène (Figure 1c) and may have occurred on top of the Mont Fort nappe farther north as well. At least, similar top-to-the-south shearing is reported from (a) greenschist facies shear zones juxtaposing the Combin zone and Zermatt-Saas zone farther to the southeast of our study area [*Cartwright and Barnicoat*, 2002; *Reddy et al.*, 2003], (b) shear zones in the Combin zone south of the Monte Rosa nappe (Gressoney shear zone introduced by *Reddy et al.* [1999]), and (c) from the base of the Austroalpine Dent Blanche-Sesia unit [e.g., *Milnes et al.*, 1981; *Müller*, 1983; *Ring*, 1995; *Lebit et al.*, 2002]. These observations indicate a regional-scale occurrence of this top-to-the-south shearing. We therefore deduce a major importance of this top-to-the-south shearing event for the general structural architecture and the development of the tectonostratigraphy of the entire area.

5.4. Possible Implications for the Tectonic Evolution of the Entire Penninic Nappe System of Western Switzerland

[64] Our observations and interpretations presented above derive from a central area within the Penninic nappe system of western Switzerland. They can be implemented into the wider tectonic framework of the Penninic system of the Western and Central Alps by considering the structural patterns of existing maps and cross sections and when taking into account available radiogenic isotope data. In Figure 12 we present a schematic tectonic evolution for the entire area. The most controversial issues are the paleogeographic and

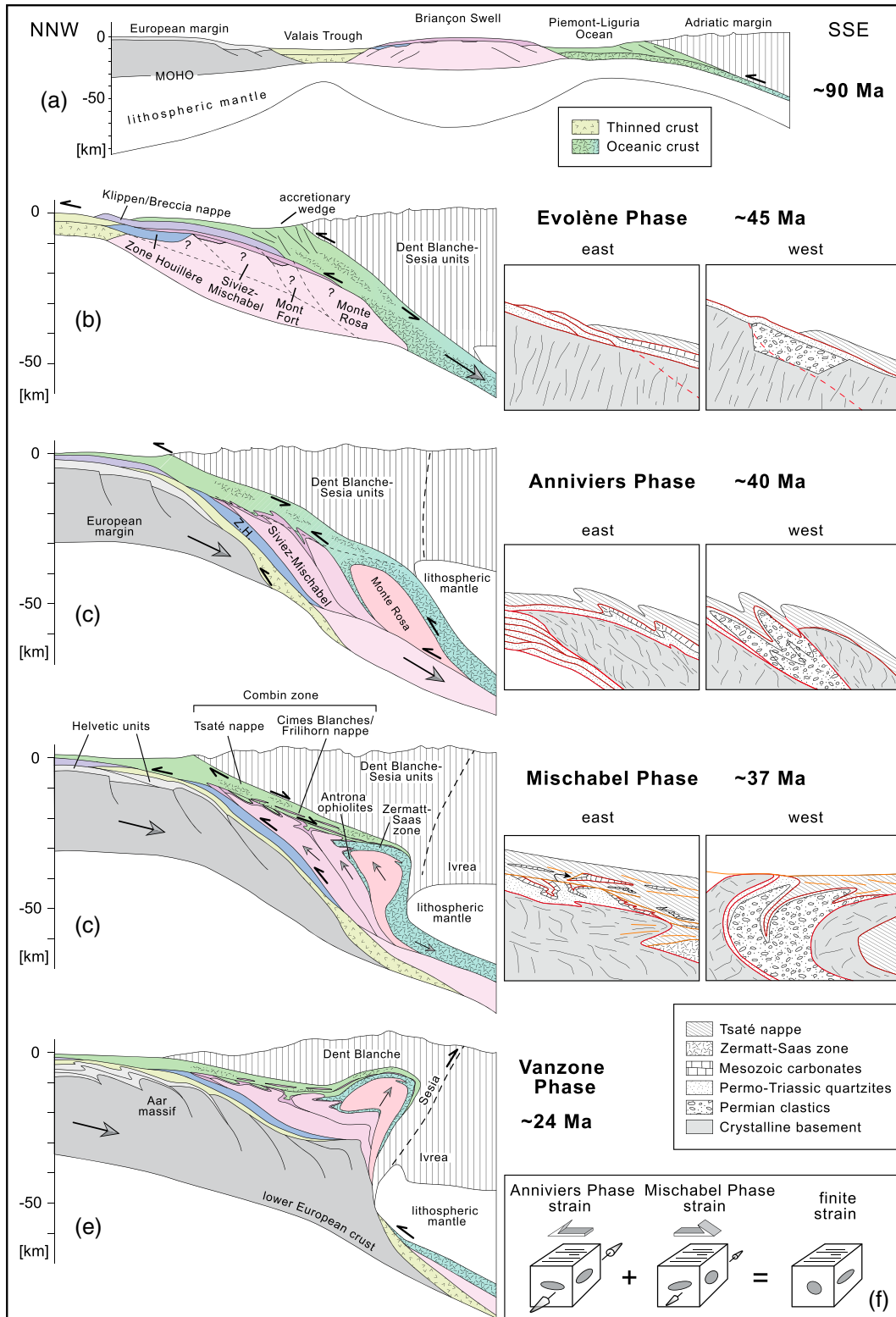


Figure 12

tectonic positions of the Antrona ophiolite and the Monte Rosa nappe [e.g., *Froitzheim, 2001* and references therein; *Keller and Schmid, 2001*; *Pleuger et al., 2005*]. For the Antrona ophiolite (Figure 1c), a Piemont-Liguria origin has traditionally been assumed [e.g., *BWG, 2005*], but a Valais origin has been proposed for structural reasons [e.g.,

Froitzheim, 2001; *Keller and Schmid, 2001*]. Radiogenic isotope dating has revealed identical Late Jurassic protolith ages for the Zermatt-Saas and Antrona ophiolites [*Rubatto et al., 1998*; *Liati et al., 2005*]. However, similar protolith ages were also obtained from the Misox zone, in the eastern Central Alps [*Liati et al., 2005*], which is generally interpreted

as Valaisan [e.g., Schmid *et al.*, 1997]. In addition, Cretaceous protolith ages (93 Ma) from the Valais-derived Chiavenna ophiolite [Liati *et al.*, 2003] are identical to the ones reported from the Balma unit on top of the Monte Rosa nappe [Liati and Froitzheim, 2006], traditionally interpreted as part of the Zermatt-Saas zone [e.g., BWG, 2005]. Thus, a protolith age-based attribution to Piemont-Liguria or Valais Ocean is not straight forward. We prefer to correlate the Zermatt-Saas zone and the Antrona ophiolite in our model and originate them in the Piemont-Liguria Ocean (Figure 12). With this choice, and with the structural evolution described in the following, the most logical place for the origin of the Monte Rosa nappe is the southern margin of the Briançon swell in our opinion (following, e.g., Escher *et al.* [1993, 1997] and Ballèvre and Merle [1993], but see Froitzheim [2001] for alternative models).

[65] With this starting configuration (Figure 12a), the first important deformation phase was the detachment and substitution of cover series in the north (e.g., thrusting of Klippen nappe, Breccia nappe, and Tsaté nappe), coeval with subduction and eclogite facies metamorphism of the Zermatt-Saas ophiolites (Evolène phase at circa 45 Ma, Figure 12b) [Rubatto *et al.*, 1998]. During the subsequent Anniviers phase at circa 40 Ma [Markley *et al.*, 1998], large-scale basement-cored folds developed at depth (folding of the Monte Rosa nappe with overlying Piemont-Liguria rocks at eclogite facies conditions), whereas thrusting was the dominant process at higher levels (e.g., frontal part of the Siviez-Mischabel nappe, Figure 12c).

[66] The next important process was backshearing and backfolding during the Mischabel phase (Figure 12d). We believe that all the top-to-the-south shear zones described in the larger area [Milnes *et al.*, 1981; Müller, 1983; Ring, 1995; Reddy *et al.*, 1999; Wheeler *et al.*, 2001; Cartwright and Barnicoat, 2002; Lebit *et al.*, 2002; Reddy *et al.*, 2003; Pleuger *et al.*, 2005, 2007; Ganne *et al.*, 2006; this study] are part of the same large-scale top-to-the-south shear system

which affected the upper part of the Briançon units and the Piemont-Liguria units during the Mischabel phase (Figure 12d). These shear zones are responsible for the juxtaposition of high-grade metamorphic rocks of the Zermatt-Saas zone next to the lower grade Combin zone and for Mischabel phase backfolding (Figure 12d). Mischabel phase backfolding affected the upper parts of the Siviez-Mischabel nappe in such a way that basement of the Siviez-Mischabel nappe was placed in contact with the Monte Rosa nappe (e.g., in the Furgg zone; see Froitzheim [2001]) and, consequently, separated the Zermatt-Saas zone from the Antrona ophiolites (Figure 1b). Interestingly, radiogenic isotope ages suggest that Anniviers phase thrusting in the north and Mischabel phase backshearing in the south partly overlap in time [Markley *et al.*, 1998; Reddy *et al.*, 1999, 2003; Cartwright and Barnicoat, 2002], indicating that the Briançon-derived stack of crystalline units mainly exhumed between an active thrust below and an active top-to-the-south low-angle fault above. A Rb/Sr, white mica age population at around 37 Ma was used to assess backshearing deformation within and especially at the base of the Combin zone [Reddy *et al.*, 2003].

[67] The subsequent Vanzone phase affected mainly the Monte Rosa nappe and adjacent units today represented by the Southern Steep Belt of the Alps [e.g., Schmid and Kissling, 2000; Pleuger *et al.*, 2008] and left minor imprints on the frontal part of the Briançon-derived nappes, which were only passively rotated into a moderately south dipping orientation (Figure 12e).

[68] The exhumation of the Monte Rosa nappe and surrounding units occurred during a time of significant erosion, the product of which accumulated in the north and south Alpine foreland basins. These foreland basins include the Molasse Basin and the Po Basin, where conglomerates accumulated in Early and Late Oligocene, respectively [Gunzenhauser, 1985; Schlunegger *et al.*, 1996; Kempf and Pfiffner, 2004; Garzanti and Malusà 2008]. Erosional

Figure 12. Schematic tectonic evolution of the western Central Alps, shown by synoptic palinspastic reconstructions at 90, 45, 40, 37, and 24 Ma. Penninic nappes are colored. Color scheme is the same as used in Figure 1b. The green gradient for Piemont-Liguria rocks indicates their metamorphic grade. Thickness of Penninic nappes is exaggerated in some cases for visualization reasons. Insets to the right show the stepwise schematic evolution of the eastern versus the western parts of the study area (not to scale). Note the scale change from Figures 12a to 12b. (a) Paleogeographic situation at 90 Ma. (b) Paleogeographic situation at 45 Ma. Evolène phase: the Briançonnais cover is largely sheared off and substituted by rocks with Piemont-Liguria origin. Note that the basal Permian to Triassic metaclastics and locally also younger carbonatic strata were not detached from their substratum. At the front of the future Siviez-Mischabel nappe: imbricate thrusting of quartzites in the east and incipient graben inversion in the west. (c) Paleogeographic situation at 40 Ma. Anniviers phase: main phase of top-to-the-NNW thrusting and folding. Penetrative deformation of the Penninic system associated with peak metamorphic conditions. Eclogite facies metamorphism affects the Monte Rosa nappe and adjacent oceanic crust. At the front of the Siviez-Mischabel nappe: isoclinal folding of the Evolène phase thrust contacts in the east and west, complex graben inversion in the west. (d) Paleogeographic situation at 37 Ma. Mischabel phase: buoyant rise of Briançon continental crust invokes top-to-the-south backshearing at the top of the nappes and backfolding, whereas top-to-the-NNW thrusting continues at the base of the nappes. A major backthrust localizes in rocks of the former Piemont-Liguria Ocean and emplaces the Combin zone (Tsaté nappe together with Frilhorn and Cimes Blanches nappes) on top of the Zermatt-Saas zone. This shear zone detaches parts of the parautochthonous Briançonnais cover, which then constitutes the Frilhorn and Cimes Blanches “nappes”. This process was observed in the east of the study area; in the west large-scale backfolding affected the whole nappe stack. (e) Paleogeographic situation at 24 Ma. Vanzone phase: thickening of the European crust, causing ongoing exhumation of Briançon units. Backfolding occurred only in the southern parts of the middle Penninic nappes. The northern parts were passively rotated into a moderately south dipping orientation. (f) Schematic strain superposition accumulated during the two main deformation phases, given for moderately deformed internal to upper parts of the Siviez-Mischabel nappe and Mont Fort nappe.

unroofing is likely to have aided the upward motion of crustal units because of load reduction as has been shown by numerical modeling [Willett *et al.*, 1993; Beaumont *et al.*, 1999; Willett, 1999; Pfiffner *et al.*, 2000].

[69] The combination of stacking of crystalline basement units along major thrusts, coeval with and followed by backfolding and reverse shearing along the upper border of these units, seems to be a fundamental process in the formation of Alpine-type continental collision zones and has also been described for the Penninic zone in eastern Switzerland [Schmid *et al.*, 1997; Scheiber *et al.*, 2012]. Reverse backfolding and backshearing may have been driven by several factors: (1) One is the buoyancy of the subducted less dense continental crust relative to the surrounding lithospheric mantle [e.g., Warren *et al.*, 2008]. Buoyant rise of light continental crust may also have aided the exhumation of more dense mafic eclogites: in our case, the buoyant Monte Rosa nappe may have been the driving factor for exhuming the mafic eclogites of the Piemont-Liguria domain on its back (Figure 12). (2) Steepening of the descending slab (rollback) may have facilitated the upward movement of light continental crust. (3) Rebound might have occurred due to the break-off of the descending Piemont-Liguria slab [von Blanckenburg and Davies, 1995].

6. Conclusions

[70] Based on our structural analysis of the central Bernard nappe complex of western Switzerland, we draw the following important conclusions: (1) The central part of the Siviez-Mischabel nappe does not constitute a simple, large-scale isoclinal fold nappe. Its structure is controlled by the presence or absence of a Permian graben infill. Where this graben was present, inversion of the graben fill caused local isoclinal folding with associated inverted limbs. Where this graben was absent, the structural style is governed by a complex thrust stack of mainly Triassic sediments. (2) The structural evolution of the Bernard nappe complex is mainly the result of three Alpine deformation phases: (i) early detachment of cover sediments during the Evolène phase, (ii) stacking of crystalline basement on top of Permo-Mesozoic sediments and graben inversion during the Anniviers phase, and (iii) backfolding and top-to-the-south shearing during the Mischabel phase. According to our observations, top-to-the-west shearing as proposed in earlier studies did not play an important role for the evolution of the central Bernard nappe complex. (3) The Mischabel phase top-to-the-south shearing described in this study might be more widespread than previously assumed: it affected large parts of the uppermost Bernard nappe complex and structurally overlying Piemont-Liguria units. It was responsible for the formation of a tectonic mélange issued from lithologies of the hanging wall and the footwall, which had previously been interpreted as allochthonous thrust sheets (the Frilhorn and possibly the Cimes Blanches “nappes”). The shear zone also juxtaposed the Combin zone (greenschist to blueschist facies metamorphism) and the Zermatt-Saas zone, which shows an eclogite facies overprint.

[71] Thus, the deformation sequence in an Alpine-type continent-continent collision zone invokes detachment, stacking, and accretion of the upper crustal layers of the subducting plate. Buoyant rise of detached crustal flakes

leads to the steepening of thrust contacts. Furthermore, foreland-directed thrusting at the base of crustal slices may be accompanied by retro shearing in structurally higher levels, which points to upward escape of the crustal material. The uppermost parts of the forelandward and upward escaping continental crust may be detached and be affected by relative backthrusting, whereas high-grade metamorphic rocks of subducted oceanic crust may also be partly exhumed on the back of such continental crustal units. This escape is further aided by erosional unroofing.

[72] **Acknowledgments.** The authors thank Hydro Exploitation SA (especially Nicola-Vittore Bretz) and Norbert SA (especially Georg Schaeren) for providing surface and subsurface data, which were an additional help for the construction of cross sections. Mario Sartori is acknowledged for guidance in the field. Field assistance by Matthias Klinkmüller, Benjamin D. Heredia, and Deta Gasser was a great help and pleasure. The manuscript benefited from careful reviews by Mario Sartori, Yves Gouffon, and Niko Froitzheim. This project was funded by the Swiss National Science Foundation (grant 200020–122143).

References

- Allimann, M. (1987), La nappe du Mont Fort dans le Val d'Hérens, *Bull. Soc. Vaud. Sc. Nat.*, 78(4), 431–444.
- Allimann, M. (1989), Les brèches de la région d'Evolène (Nappe du Mont Fort, Valais, Suisse), *Schweiz. Mineral. Petrogr. Mitt.*, 69(2), 237–250, doi:10.5169/seals-52791.
- Argand, E. (1909), L'exploration géologique des Alpes Pennines Centrales, *Bull. Soc. Vaud. Sc. Nat.*, 166, 65 pp.
- Argand, E. (1916), Sur l'arc des Alpes Occidentales, *Ecologae Geol. Helv.*, 14(1), 145–204, doi:10.5169/seals-157596.
- Ballèvre, M., and O. Merle (1993), The Combin Fault: Compressional reactivation of a Late Cretaceous-Early Tertiary detachment fault in the Western Alps, *Schweiz. Mineral. Petrogr. Mitt.*, 73(2), 205–227, doi:10.5169/seals-55570.
- Barnicoat, A. C., D. C. Rex, P. G. Guise, and R. A. Cliff (1995), The timing of and nature of greenschist facies deformation and metamorphism in the upper Pennine Alps, *Tectonics*, 14(2), 279–293.
- Baud, A., and M. Septfontaine (1980), Présentation d'un profil palinspastique de la nappe des Préalpes médianes en Suisse occidentale, *Ecologae Geol. Helv.*, 73, 651–660, doi:10.5169/seals-164982.
- Bearth, P. (1963), Contribution à la subdivision tectonique et stratigraphique du Cristallin de la nappe du Grand-St-Bernard dans le Valais (Suisse), in *Livre à la Mémoire du Professeur Paul Fallot*, edited by M. Durand Delga, pp. 407–418, Mémoire hors-série, Société géologique de France, t. II, (1960-1963), Paris.
- Beaumont, C., S. Ellis, and A. Pfiffner (1999), Dynamics of sediment subduction-accretion at convergent margins: Short-term modes, long-term deformation, and tectonic implications, *J. Geophys. Res.*, 104, 573–601.
- Beltrando, M., D. Rubatto, and G. Manatschal (2010), From passive margins to orogens: The link between ocean-continent transition zones and (ultra)high-pressure metamorphism, *Geology*, 38(6), 559–562, doi:10.1130/g30768.1.
- von Blanckenburg, F., and J. H. Davies (1995), Slab breakoff: A model for syncollisional magmatism and tectonics in the Alps, *Tectonics*, 14(1), 120–131.
- Bousquet, R., M. Engi, G. Gosso, R. Oberhänsli, A. Berger, M. I. Spalla, M. Zucali, and B. Goffé (2004), Explanatory notes to the map: Metamorphic structure of the Alps. Transition from the western to the central Alps, *Mitt. Österr. Miner. Ges.*, 149, 145–156.
- Bucher, S., C. Ulardic, R. Bousquet, S. Ceriani, B. Fugenschuh, Y. Gouffon, and S. M. Schmid (2004), Tectonic evolution of the Briançonnais units along a transect (ECORS-CROP) through the Italian-French Western Alps, *Ecologae Geol. Helv.*, 97(3), 321–345, doi:10.1007/s00015-004-1139-0.
- Burri, M. (1983), Le front du Grand St-Bernard du val d'Hérens au val d'Aoste, *Ecologae Geol. Helv.*, 76(3), 469–490, doi:10.5169/seals-165373.
- Bussy, F., M. H. Derron, J. Jacquod, M. Sartori, and P. Thélin (1996a), The 500 Ma-old Thyon metagranite: A new A-type granite occurrence in the western Penninic Alps (Wallis, Switzerland), *Eur. J. Mineral.*, 8, 565–575.
- Bussy, F., M. Sartori, and P. Thélin (1996b), U-Pb zircon dating in the middle Penninic basement of the Western Alps (Valais, Switzerland), *Schweiz. Mineral. Petrogr. Mitt.*, 76(1), 81–84, doi:10.5169/seals-57689.
- BWG (2005), Tektonische Karte der Schweiz, *Tectonic map of Switzerland* 1:500,000, Bundesamt für Wasser und Geologie, ern.
- Campani, M., N. Mancktelow, D. Seward, Y. Rolland, W. Muller, and I. Guerra (2010), Geochronological evidence for continuous exhumation

- through the ductile-brittle transition along a crustal-scale low-angle normal fault: Simplon Fault Zone, central Alps, *Tectonics*, 29, TC3002, doi:10.1029/2009TC002582.
- Cartwright, I., and A. C. Barnicoat (2002), Petrology, geochronology, and tectonics of shear zones in the Zermatt–Saas and Combin zones of the Western Alps, *J. Metamorph. Geol.*, 20(2), 263–281, doi:10.1046/j.0263-4929.2001.00366.x.
- Champagnac, J.-D., C. Sue, and B. Delacou (2003), Brittle orogen-parallel extension in the internal zones of the Swiss Alps (South Valais), *Eclogae Geol. Helv.*, 96(3), 325–338.
- Chopin, C., B. Goffé, L. Ungaretti, and R. Oberti (2003), Magnesio-stauriolite and zincostauriolite: Mineral description with a petrogenetic and crystal-chemical update, *Eur. J. Mineral.*, 15(1), 167–176, doi:10.1127/0935-1221/2003/0015-0167.
- Desmons, J. (1992), The Briançon basement (Pennine Western Alps): Mineral composition and polymetamorphic evolution, *Schweiz. Mineral. Petrogr. Mitt.*, 72(1), 37–55, doi:10.5169/seals-54894.
- Desmons, J., R. Compagnoni, L. Cortesogno, M. Frey, and L. Gaggero (1999), Pre-alpine metamorphism of the internal zones of the Western Alps, *Schweiz. Mineral. Petrogr. Mitt.*, 79(1), 23–39, doi:10.5169/seals-60196.
- Deville, E., S. Fudral, Y. Lagabrielle, M. Marthaler, and M. Sartori (1992), From oceanic closure to continental collision: A synthesis of the “Schistes lustrés” metamorphic complex of the Western Alps, *Geol. Soc. Am. Bull.*, 104(2), 127–139, doi:10.1130/0016-7606(1992)104<0127:focct>2.3.co;2.
- Eisele, J., S. Geiger, and M. Rahn (1997), Chemical characterization of metabasites from the Turtmanntal valley (Valais, Switzerland): Implications for their protoliths and geotectonic origin, *Schweiz. Mineral. Petrogr. Mitt.*, 77(3), 403–417, doi:10.5169/seals-58493.
- Ellenberger, F. (1952), Sur l’extension des faciès Briançonnais en Suisse, dans les Préalpes médianes et les Pennides, *Eclogae Geol. Helv.*, 45(2), 285–286.
- Ellenberger, F. (1953), La Série du Barrhorn et les rétrocharrages penniques, *Comptes Rendus de l’Académie des sciences*, 236, 218–220.
- Epard, J.-L., and A. Escher (1996), Transition from basement to cover: A geometric model, *J. Struct. Geol.*, 18(5), 533–548, doi:10.1016/S0191-8141(96)80022-8.
- Escher, A. (1988), Structure de la nappe du Grand Saint-Bernard entre le val de Bagnes et les Mischabel, *Rapport géologique du Service hydrologique et géologique national*, 7.
- Escher, A., and C. Beaumont (1997), Formation, burial and exhumation of basement nappes at crustal scale: A geometric model based on the Western Swiss-Italian Alps, *J. Struct. Geol.*, 19(7), 955–974, doi:10.1016/S0191-8141(97)00022-9.
- Escher, A., H. Masson, and A. Steck (1988), Coupes géologiques des Alpes occidentales suisses, *Mémoires de Géologie Lausanne*, 2.
- Escher, A., H. Masson, and A. Steck (1993), Nappe geometry in the Western Swiss Alps, *J. Struct. Geol.*, 15(3–5), 501–509, doi:10.1016/0191-8141(93)90144-Y.
- Escher, A., J. C. Hunziker, M. Marthaler, H. Masson, M. Sartori, and A. Steck (1997), Geologic framework and structural evolution of the western Swiss-Italian Alps, in *Deep Structure of the Swiss Alps: Results of NRP 20*, edited by O. A. Pfiffner et al., pp. 205–221, Birkhäuser Verlag, Basel, Boston, Berlin.
- Forster, M. A., and G. S. Lister (2008), Tectonic sequence diagrams and the structural evolution of schists and gneisses in multiply deformed terranes, *J. Geol. Soc.*, 165(5), 923–939, doi:10.1144/0016-76492007-016.
- Frezza, M. L., J. Selverstone, Z. D. Sharp, and R. Compagnoni (2011), Carbonate dissolution during subduction revealed by diamond-bearing rocks from the Alps, *Nat. Geosci.*, 4(10), 703–706, doi:10.1038/NGEO1246.
- Froitzheim, N. (2001), Origin of the Monte Rosa nappe in the Pennine Alps—A new working hypothesis, *Geol. Soc. Am. Bull.*, 113(5), 604–614, doi:10.1130/0016-7606(2001)113<0604:OOTMRN>2.0.CO;2.
- Froitzheim, N., J. Pleuger, and T. J. Nagel (2006), Extraction faults, *J. Geol. Soc.*, 28(8), 1388–1395, doi:10.1016/j.jsg.2006.05.002.
- Gabus, J. H., M. Weidmann, P.-C. Bugnon, M. Burri, M. Sartori, and M. Marthaler (2008a), Feuille 1287 Sierre, *Atlas géologique de la Suisse* 1:25,000, Carte 111, swisstopo, Wabern.
- Gabus, J. H., M. Weidmann, M. Burri, and M. Sartori (2008b), Feuille 1287 Sierre, *Atlas géologique de la Suisse* 1:25,000, Carte 111, Notice explicative, swisstopo, Wabern.
- Ganne, J., D. Marquer, G. Rosenbaum, J.-M. Bertrand, and S. Fudral (2006), Partitioning of deformation within a subduction channel during exhumation of high-pressure rocks: A case study from the Western Alps, *J. Struct. Geol.*, 28(7), 1193–1207, doi:10.1016/j.jsg.2006.02.011.
- Garzanti, E., and M. G. Malusà (2008), The Oligocene Alps: Domal unroofing and drainage development during early orogenic growth, *Earth Planet. Sci. Lett.*, 268(3–4), 487–500, doi:10.1016/j.epsl.2008.01.039.
- Gauthiez, L., F. Bussy, A. Ulianov, Y. Gouffon, and M. Sartori (2011), Ordovician mafic magmatism in the Métallifer Formation of the Mont-Fort nappe (Middle Penninic domain, western Alps)—Geodynamic implications, paper presented at 9th Swiss Geoscience Meeting, Zürich, Switzerland.
- Genier, F. (2007), Structure and kinematics of the Siviez-Mischabel nappe in the Matteral (western Alps of Switzerland), Ph.D. thesis, Univ. de Lausanne, Switzerland.
- Genier, F., J.-L. Epard, F. Bussy, and T. Magna (2008), Lithostratigraphy and U-Pb zircon dating in the overturned limb of the Siviez-Mischabel nappe: A new key for Middle Penninic nappe geometry, *Swiss J. Geosci.*, 101(2), 431–452, doi:10.1007/s00015-008-1261-5.
- Giorgis, D., P. Thélin, G. M. Stampfli, and F. Bussy (1999), The Mont-Mort metapelites: Variscan metamorphism and geodynamic context (Briançonnais basement, Western Alps, Switzerland), *Schweiz. Mineral. Petrogr. Mitt.*, 79(3), 381–389, doi:10.5169/seals-60214.
- Göksu, E. (1947), Geologische Untersuchungen zwischen Val d’Anniviers und Turtmanntal (Wallis), Ph.D. thesis, ETH Zürich, Switzerland.
- Gouffon, Y., and M. Burri (1997), Les nappes des Pontis, de Siviez-Mischabel et du Mont Fort dans les vallées de Bagnes, d’Entremont (Valais, Suisse) et d’Aoste (Italie), *Eclogae Geol. Helv.*, 90(1), 29–41, doi:10.5169/seals-168143.
- Gunzenhauser, B. A. (1985), Zur Sedimentologie und Paläogeographie der oligo-miocänen Gonfolite Lombarda zwischen Lago Maggiore und der Brianza (Südtessin, Lombardei), *Beiträge zur Geologischen Karte der Schweiz, N.F. 159*, 114 pp.
- Hermann, F.-W. (1913), Recherches géologiques dans la partie septentrionale des Alpes pennines (massifs Rocs de Boudri—Bella Tola et Sasseneire-Becc de Bosson). Levés géologiques 1909-1910, Ph.D. thesis, Univ. de Lyon, France.
- Hunziker, J. C. (1969), Rb-Sr-Altersbestimmungen aus den Walliser Alpen: Hellglimmer- und Gesamtgesteinsalterswerte, *Eclogae Geol. Helv.*, 62(2), 527–542, doi:10.5169/seals-163710.
- Hunziker, J., and P. Bearth (1969), Rb-Sr-Altersbestimmungen aus den Walliser Alpen: Biotitalterswerte und ihre Bedeutung für die Abkühlungsgeschichte der alpinen Metamorphose, *Eclogae Geol. Helv.*, 62(1), 205–222, doi:10.5169/seals-163698.
- Jäckli, R. (1950), Geologische Untersuchungen in der Stirnzone der Mischabeldecke zwischen Réchy, Val d’Anniviers und Visp (Wallis), *Eclogae Geol. Helv.*, 43(1), 31–93, doi:10.5169/seals-161304.
- Jeanbourquin, P., and M. Burri (1991), Les métasédiments du Pennique inférieur dans la région de Brigue-Simplon: Lithostratigraphie, structure et contexte géodynamique dans le bassin Valaisan, *Eclogae Geol. Helv.*, 84(2), 463–481, doi:10.5169/seals-166785.
- Keller, L. M., and S. M. Schmid (2001), On the kinematics of shearing near the top of the Monte Rosa nappe and the nature of the Furgg zone in Val Loranco (Antrona valley, N. Italy): Tectonometamorphic and paleogeographical consequences, *Schweiz. Mineral. Petrogr. Mitt.*, 81(3), 347–367, doi:10.5169/seals-61697.
- Kempf, O., and O. A. Pfiffner (2004), Early Tertiary evolution of the North Alpine Foreland Basin of the Swiss Alps and adjoining areas, *Basin Res.*, 16(4), 549–567, doi:10.1111/j.1365-2117.2004.00246.x.
- Klein, J. A. (1978), Post-nappe folding southeast of the Mischabelrückfalte (Pennine Alps) and some aspects of the associated metamorphism, *Leidse Geologische Mededelingen*, 51, 233–312.
- Kramer, N., M. A. Cosca, and J. C. Hunziker (2001), Heterogeneous 40Ar* distributions in naturally deformed muscovite: In situ UV-laser ablation evidence for microstructurally controlled intragrain diffusion, *Earth Planet. Sci. Lett.*, 192(3), 377–388, doi:10.1016/S0012-821X(01)00456-3.
- Kramer, J. (2002), Structural evolution of the Penninic units in the Monte Rosa region (Swiss and Italian Alps), Ph.D. thesis, Univ. Basel, Switzerland.
- Lapen, T. J., C. M. Johnson, L. P. Baumgartner, N. J. Mahlen, B. L. Beard, and J. M. Amato (2003), Burial rates during prograde metamorphism of an ultra-high-pressure terrane: An example from Lago di Cignana, western Alps, Italy, *Earth Planet. Sci. Lett.*, 215(1–2), 57–72, doi:10.1016/S0012-821X(03)00455-2.
- Lapen, T. J., C. M. Johnson, L. P. Baumgartner, G. V. Dal Piaz, S. Skora, and B. L. Beard (2007), Coupling of oceanic and continental crust during Eocene eclogite-facies metamorphism: Evidence from the Monte Rosa nappe, western Alps, *Contrib. Mineral. Petrol.*, 153(2), 139–157, doi:10.1007/s00410-006-0144-x.
- Lebit, H., E. M. Klaper, and C. M. Lüneburg (2002), Fold-controlled quartz textures in the Pennine Mischabel backfold near Zermatt, Switzerland, *Tectonophysics*, 359(1–2), 1–28, doi:10.1016/S0040-1951(02)00387-6.
- Lemoine, M. (1960), Sur les caractères stratigraphiques et l’ordre de succession des unités à la marge interne de la zone Briançonnaise, *Comptes Rendus Société Géologique de France*, 5, 9–97.
- Liati, A., and N. Froitzheim (2006), Assessing the Valais Ocean, Western Alps: U-Pb SHRIMP zircon geochronology of eclogite in the Balma unit, on top of the Monte Rosa nappe, *Eur. J. Mineral.*, 18(3), 299–308, doi:10.1127/0935-1221/2006/0018-0299.
- Liati, A., D. Gebauer, and C. M. Fanning (2003), The youngest basic oceanic magmatism in the Alps (Late Cretaceous: Chiavenna unit, Central Alps): Geochronological constraints and geodynamic significance, *Contrib. Mineral. Petrol.*, 146(2), 144–158, doi:10.1007/s00410-003-0485-7.

- Liati, A., N. Froitzheim, and C. M. Fanning (2005), Jurassic ophiolites within the Valais domain of the Western and Central Alps: Geochronological evidence for re-rifting of oceanic crust, *Contrib. Mineral. Petrol.*, 149(4), 446–461, doi:10.1007/s00410-005-0658-7.
- Mancktelow, N. (1985), The Simplon Line: a major displacement zone in the western Lepontine Alps, *Eclogae Geol. Helv.*, 78(1), 73–96, doi:10.5169/seals-165644.
- Mancktelow, N. S. (1992), Neogene lateral extension during convergence in the Central Alps—Evidence from interrelated faulting and backfolding around the Simplonpass (Switzerland), *Tectonophysics*, 215(3–4), 295–317.
- Markley, M. J., C. Teyssier, M. A. Cosca, R. Caby, J. C. Hunziker, and M. Sartori (1998), Alpine deformation and $40\text{Ar}/39\text{Ar}$ geochronology of synkinematic white mica in the Siviez-Mischabel Nappe, western Pennine Alps, Switzerland, *Tectonics*, 17(3), 407–425.
- Markley, M. J., C. Teyssier, and R. Caby (1999), Re-examining Argand's view of the Siviez-Mischabel nappe, *J. Struct. Geol.*, 21(8–9), 1119–1124, doi:10.1016/S0191-8141(99)00063-2.
- Markley, M. J., C. Teyssier, and M. Cosca (2002), The relation between grain size and $40\text{Ar}/39\text{Ar}$ date for Alpine white mica from the Siviez-Mischabel Nappe, Switzerland, *J. Struct. Geol.*, 24(12), 1937–1955, doi:10.1016/S0191-8141(02)00006-8.
- Marthaler, M. (1984), Géologie des unités penniques entre le val d'Anniviers et le val de Tourtemagne (Valais, Suisse), *Eclogae Geol. Helv.*, 77(2), 395–448, doi:10.5169/seals-165516.
- Marthaler, M., and G. M. Stampfli (1989), Les Schistes lustrés à ophiolites de la nappe du Tsaté: Un ancien prisme d'accrétion issu de la marge active apulienne?, *Schweiz. Mineral. Petrogr. Mitt.*, 69(2), 211–216, doi:10.5169/seals-52789.
- Marthaler, M., M. Sartori, and A. Escher (2008a), Feuille 1307 Vissoie, *Atlas géologique de la Suisse 1:25,000*, Carte 122, swisstopo, Wabern.
- Marthaler, M., M. Sartori, A. Escher, and N. Meisser (2008b), Feuille 1307 Vissoie, *Atlas géologique de la Suisse 1:25,000*, Carte 122, Notice explicative, swisstopo, Wabern.
- Masson, H., A. Baud, and A. Escher (1980), Compte rendu de l'excursion de la Société Géologique Suisse du 1 au 3 octobre 1979: Coupe Préalpes-Helvétique-Pennique en Suisse occidentale, *Eclogae Geol. Helv.*, 73(1), 331–349, doi:10.5169/seals-164959.
- Milnes, A. G., M. Grellier, and R. Müller (1981), Sequence and style of major post-nappe structures, Simplon-Pennine Alps, *J. Struct. Geol.*, 3(4), 411–420, doi:10.1016/0191-8141(81)90041-9.
- Müller, R. (1983), Die Struktur der Mischabelfalte (Penninische Alpen), *Eclogae Geol. Helv.*, 76(2), 391–416, doi:10.5169/seals-165369.
- Oberhänsli, R., et al. (2004), Metamorphic structure of the Alps, *Commission for the Geological Map of the World 1:1,000,000*, sGMW, Paris.
- Pfiffner, O. A., S. Ellis, and C. Beaumont (2000), Collision tectonics in the Swiss Alps: Insight from geodynamic modeling, *Tectonics*, 19(6), 1065–1094.
- Pleuger, J., N. Froitzheim, and E. Jansen (2005), Folded continental and oceanic nappes on the southern side of Monte Rosa (western Alps, Italy): Anatomy of a double collision suture, *Tectonics*, 24(4), TC4013, doi:10.1029/2004TC001737.
- Pleuger, J., S. Roller, J. Walter, E. Jansen, and N. Froitzheim (2007), Structural evolution of the contact between two Penninic nappes (Zermatt-Saas zone and Combin zone, Western Alps) and implications for the exhumation mechanism and palaeogeography, *Int. J. Earth Sci.*, 96(2), 229–252, doi:10.1007/s00531-006-0106-6.
- Pleuger, J., T. J. Nagel, J. M. Walter, E. Jansen, and N. Froitzheim (2008), On the role and importance of orogen-parallel and -perpendicular extension, transcurrent shearing, and backthrusting in the Monte Rosa nappe and the Southern Steep Belt of the Alps (Penninic zone, Switzerland and Italy), *Geological Society, London, Special Publications*, 298, 251–280, doi:10.1144/sp298.13.
- Rahn, M. (1991), Eclogites from the Minugrat, Siviez-Mischabel nappe (Valais, Switzerland), *Schweiz. Mineral. Petrogr. Mitt.*, 71(3), 415–426, doi:10.5169/seals-54374.
- Reddy, S. M., J. Wheeler, and R. A. Cliff (1999), The geometry and timing of orogenic extension: An example from the Western Italian Alps, *J. Metamorph. Geol.*, 17(5), 573–589, doi:10.1046/j.1525-1314.1999.00220.x.
- Reddy, S. M., J. Wheeler, R. W. H. Butler, R. A. Cliff, S. Freeman, S. Inger, C. Pickles, and S. P. Kelley (2003), Kinematic reworking and exhumation within the convergent Alpine Orogen, *Tectonophysics*, 365(1–4), 77–102, doi:10.1016/S0040-1951(03)00017-9.
- Ring, U. (1995), Horizontal contraction or horizontal extension? Heterogeneous Late Eocene and early Oligocene general shearing during blueschist and greenschist facies metamorphism at the Pennine-Austroalpine boundary zone in the Western Alps, *Geol. Rundsch.*, 84(4), 843–859, doi:10.1007/bf00240572.
- Rubatto, D., D. Gebauer, and M. Fanning (1998), Jurassic formation and Eocene subduction of the Zermatt-Saas-Fee ophiolites: Implications for the geodynamic evolution of the Central and Western Alps, *Contrib. Mineral. Petrol.*, 132(3), 269–287, doi:10.1007/s004100050421.
- Sartori, M. (1987a), Structure de la zone du Combin entre les Diablons et Zermatt (Valais), *Eclogae Geol. Helv.*, 80(3), 789–814, doi:10.5169/seals-166026.
- Sartori, M. (1987b), Blocs basculés briançonnais en relation avec leur socle original dans la nappe de Siviez-Mischabel (Valais, Suisse), *Comptes Rendus de l'Académie des sciences*, 305(2), 999–1005.
- Sartori, M. (1990), L'unité du Barrhorn (Zone pennique, Valais, Suisse), *Mémoires de Géologie, Lausanne*, 6, 156.
- Sartori, M., and J. L. Epard (2011), Feuille 1306 Sion, *Atlas géologique de la Suisse 1:25,000*, Carte 130, Notice explicative, swisstopo, Wabern.
- Sartori, M., and M. Marthaler (1994), Exemples de relations socle-couverture dans les nappes penniques du Val d'Hérens: Compte-rendu de l'excursion de la Société Géologique Suisse et de la Société Suisse de Minéralogie et Pétrographie (25 et 26 septembre 1993), *Schweiz. Mineral. Petrogr. Mitt.*, 74(3), 503–509, doi:10.5169/seals-56365.
- Sartori, M., and P. Thélin (1987), Les schistes ocellés albitiques de Barneua (Nappe de Siviez-Mischabel, Valais, Suisse), *Schweiz. Mineral. Petrogr. Mitt.*, 67(3), 229–256, doi:10.5169/seals-51602.
- Sartori, M., Y. Gouffon, and M. Marthaler (2006), Harmonisation et définition des unités lithostratigraphiques briançonnaises dans les nappes penniques du Valais, *Eclogae Geol. Helv.*, 99(3), 363–407, doi:10.1007/s00015-006-1200-2.
- Sartori, M., M. Burri, J. L. Epard, H. Masson, and J. B. Pasquier (2011), Feuille 1306 Sion, *Atlas géologique de la Suisse 1:25,000*, Carte 130, swisstopo, Wabern.
- Savary, J., and B. Schneider (1983), Déformations superposées dans les Schistes lustrés et les Ophiolites du val d'Hérens (Valais), *Eclogae Geol. Helv.*, 76(2), 381–389, doi:10.5169/seals-165368.
- Schaad, W. (1995), Beiträge zur Entstehung und Bedeutung alpintektonischer Abscherhorizonte in den Schweizer Alpen, Ph.D. thesis, Univ. of Bern, Switzerland.
- Schaer, J.-P. (1959), Géologie de la partie septentrionale de l'éventail de Bagnes, *Archives des Sciences, Genève*, 12(4), 473–620.
- Scheiber, T., O. A. Pfiffner, and G. Schreurs (2012), Strain accumulation during basal accretion in continental collision—A case study from the Suretta nappe (eastern Swiss Alps), *Tectonophysics*, 579, 56–73, doi:10.1016/j.tecto.2012.03.009.
- Schlunegger, F., D. W. Burbank, and A. Matter (1996), Magnetostratigraphic calibration of the Oligocene to Middle Miocene (30–15 Ma) mammal biozones and depositional sequences of the Swiss Molasse Basin, *Eclogae Geol. Helv.*, 89(2), 753–788, doi:10.5169/seals-167923.
- Schmid, S. M., and E. Kissling (2000), The arc of the western Alps in the light of geophysical data on deep crustal structure, *Tectonics*, 19(1), 62–85.
- Schmid, S. M., O. A. Pfiffner, and G. Schreurs (1997), Rifting and collision in the Penninic zone of eastern Switzerland, in *Deep Structure of the Swiss Alps: Results of NRP 20*, edited by O. A. Pfiffner et al., pp. 160–185, Birkhäuser Verlag, Basel, Boston, Berlin.
- Schmid, S. M., B. Fügenschuh, E. Kissling, and R. Schuster (2004), Tectonic map and overall architecture of the Alpine orogen, *Eclogae Geol. Helv.*, 97(1), 93–117, doi:10.1007/s00015-004-1113-x.
- Soom, M. (1990), Abkühlungs- und Hebungsgeschichte der Externmassive und der penninischen Decken beidseits der Simplon-Rhone-Linie seit dem Oligozän: Spaltspurdaterungen an Apatit/Zirkon und K-Ar-Datierungen an Biotit/Muskowit (Westliche Zentralalpen), Ph.D. thesis, Univ. Bern, Switzerland.
- Stampfli, G. M. (1993), Le Briançonnais, terrain exotique dans les Alpes?, *Eclogae Geol. Helv.*, 86(1), 1–45, doi:10.5169/seals-167234.
- Stampfli, G. M., J. Mosar, D. Marquer, R. Marchant, T. Baudin, and G. Borel (1998), Subduction and obduction processes in the Swiss Alps, *Tectonophysics*, 296(1–2), 159–204, doi:10.1016/S0040-1951(98)00142-5.
- Staub, R. (1937), Gedanken zum Bau der Westalpen zwischen Bernina und Mittelmeer. 1. Teil, *Vierteljahrsschr. Natf. Ges. Zürich*, 82, 1–100.
- Steck, A. (1984), Structures de déformations tertiaires dans les Alpes centrales, *Eclogae Geol. Helv.*, 77(1), 55–100, doi:10.5169/seals-165499.
- Steck, A. (1990), Une carte des zones de cisaillement ductile des Alpes Centrales, *Eclogae Geol. Helv.*, 83(3), 603–627, doi:10.5169/seals-166604.
- Steck, A. (2008), Tectonics of the Simplon massif and Lepontine gneiss dome: Deformation structures due to collision between the underthrusting European plate and the Adriatic indenter, *Swiss J. Geosci.*, 101(2), 515–546, doi:10.1007/s00015-008-1283-z.
- Steck, A., B. Bigoggero, G. V. dal Piaz, A. Escher, G. Martinotti, and H. Masson (1999), Carte tectonique des Alpes de Suisse occidentale, *Carte géologique spéciale 1:100,000*, N° 123, Service hydrologique et géologique national, Bern.
- Steck, A., J. L. Epard, A. Escher, Y. Gouffon, and H. Masson (2001), Notice explicative de la Carte tectonique des Alpes de Suisse occidentale et des régions avoisinantes 1:100,000, *Carte géologique spéciale*, N° 123, Office féd. Eaux Géologie, Bern.
- Thélin, P. (1987), Nature originelle des gneiss ocellés de Randa (Nappe de Siviez-Mischabel, Valais), *Mém. Soc. Vaud. Sci. Nat.* No. 104, 18, 75 pp.

- Thélin, P. (1989), Essai de chronologie magmatico-métamorphique dans le socle de la nappe du Grand Saint-Bernard: Quelques points de repère, *Schweiz. Mineral. Petrogr. Mitt.*, 69(2), 193–204, doi:10.5169/seals-52787.
- Thélin, P., and S. Ayrton (1983), Cadre évolutif des événements magmatico-métamorphiques du socle anté-triasique dans le domaine pennique (Valais), *Schweiz. Mineral. Petrogr. Mitt.*, 63(2), 393–420, doi:10.5169/seals-48743.
- Thélin, P., M. Sartori, R. Lengeler, and J.-P. Schaerer (1990), Eclogites of Paleozoic or early Alpine age in the basement of the Penninic Siviez-Mischabel nappe, Wallis, Switzerland, *Lithos*, 25(1-3), 71–88, doi:10.1016/0024-4937(90)90007-N.
- Thélin, P., M. Sartori, M. Burri, Y. Gouffon, and R. Chessex (1993), The pre-Alpine basement of the Briançonnais (Wallis, Switzerland), in *Pre-Mesozoic Geology in the Alps*, edited by J. F. von Raumer and F. Neubauer, pp. 297–315, Springer, Berlin.
- Trümpy, R. (1951), Sur les racines helvétiques et les “Schistes lustrés” entre le Rhône et la Vallée de Bagnes (Région de la Pierre Avoi), *Eclogae Geol. Helv.*, 44(2), 338–347.
- Vallet, J.-M. (1950), Etude géologique et pétrographique de la partie inférieure du Val d’Hérens et du Val d’Héremence (Valais), *Schweiz. Mineral. Petrogr. Mitt.*, 30(2), 322–476, doi:10.5169/seals-24449.
- Vannay, J. C., and R. Allemann (1990), La zone piémontaise dans le Haut-Valtournanche (Val d’Aoste, Italie), *Eclogae Geol. Helv.*, 83(1), 21–39, doi:10.5169/seals-166575.
- Warren, C. J., C. Beaumont, and R. A. Jamieson (2008), Modelling tectonic styles and ultra-high pressure (UHP) rock exhumation during the transition from oceanic subduction to continental collision, *Earth Planet. Sci. Lett.*, 267(1-2), 129–145, doi:10.1016/j.epsl.2007.11.025.
- Wegmann, E. (1923), Zur Geologie der St. Bernharddecke im Val D’Hérens (Wallis), Ph.D. thesis, Univ. de Neuchâtel, Switzerland.
- Wheeler, J., S. M. Reddy, and R. A. Cliff (2001), Kinematic linkage between internal zone extension and shortening in more external units in the NW Alps, *J. Geol. Soc.*, 158(3), 439–443, doi:10.1144/jgs.158.3.439.
- Willett, S. D. (1999), Orogeny and orography: The effects of erosion on the structure of mountain belts, *J. Geophys. Res.*, 104(B12), 957–981, doi:10.1029/1999jb900248.
- Willett, S., C. Beaumont, and P. Fullsack (1993), Mechanical model for the tectonics of doubly vergent compressional orogens, *Geology*, 21(4), 371–374, doi:10.1130/0091-7613(1993)021<0371:mmftto>2.3.co;2.
- Witzig, E. (1948), Geologische Untersuchungen in der Zone du Combin im Val des Dix (Wallis), Ph.D. thesis, ETH Zürich, Switzerland.